

5-1-2024

Spatially Fractionated Radiation Therapy Implementation At Intermountain Cancer Center

Anupreet Kaur

Follow this and additional works at: <https://digitalscholarship.unlv.edu/thesesdissertations>



Part of the [Medicine and Health Sciences Commons](#)

Repository Citation

Kaur, Anupreet, "Spatially Fractionated Radiation Therapy Implementation At Intermountain Cancer Center" (2024). *UNLV Theses, Dissertations, Professional Papers, and Capstones*. 5019.
<http://dx.doi.org/10.34917/37650842>

This Dissertation is protected by copyright and/or related rights. It has been brought to you by Digital Scholarship@UNLV with permission from the rights-holder(s). You are free to use this Dissertation in any way that is permitted by the copyright and related rights legislation that applies to your use. For other uses you need to obtain permission from the rights-holder(s) directly, unless additional rights are indicated by a Creative Commons license in the record and/or on the work itself.

This Dissertation has been accepted for inclusion in UNLV Theses, Dissertations, Professional Papers, and Capstones by an authorized administrator of Digital Scholarship@UNLV. For more information, please contact digitalscholarship@unlv.edu.

SPATIALLY FRACTIONATED RADIATION THERAPY IMPLEMENTATION AT
INTERMOUNTAIN CANCER CENTER

By

Anupreet Kaur

Bachelor of Science – Physics
Panjab University
2008

Master of Science – Physics
Panjab University
2010

Bachelor of Education
Punjabi University
2012

Master of Science – Medical Physics
San Diego State University
2018

A doctoral project submitted in partial fulfillment
of the requirements for the

Doctor of Medical Physics

Department of Health Physics and Diagnostic Sciences
School of Integrated Health Sciences
The Graduate College

University of Nevada, Las Vegas
May 2024

March 27, 2024

This doctoral project prepared by

Anupreet Kaur

entitled

Spatially Fractionated Radiation Therapy Implementation At Intermountain Cancer
Center

is approved in partial fulfillment of the requirements for the degree of

Doctor of Medical Physics
Department of Health Physics and Diagnostic Sciences

Steen Madsen, Ph.D.
Examination Committee Chair

Alyssa Crittenden, Ph.D.
*Vice Provost for Graduate Education &
Dean of the Graduate College*

Yu Kuang, Ph.D.
Examination Committee Member

Cephas Mubata, Ph.D.
Examination Committee Member

David Zhang, Ph.D.
Examination Committee Member

Ryan Hecox, Ph.D.
Examination Committee Member

James Navalta, Ph.D.
Graduate College Faculty Representative

ABSTRACT

Spatially Fractionated Radiation Therapy (SFRT) is a treatment method that distributes a non-uniform dose with alternating peaks and valleys within a tumor. It is an effective technique to treat large and bulky tumors with limited toxicity to surrounding Organs At Risk (OAR), which is normally hard to treat using traditional radiation therapy methods. It can either be delivered by using a three-dimensional conformal planning technique (either physical block or virtually using Multi Leaf Collimators (MLC)), or by Lattice Radiation Therapy (LRT) using Volumetric Modulated Arc Therapy (VMAT) technique. The scope of this work is to compare and implement SFRT treatment techniques at Intermountain Cancer Center (ICC). This requires the investigation of physical and dosimetric characteristics of the grid, describing its clinical implementation and verification, creating treatment plans on test patients using different methods of SFRT, assessment of the parameters that decides the acceptability of the plan, establishing Quality Assurance (QA) methods, and making recommendations about treatment planning and dose reporting. All the measurement results for SFRT commissioning were found to be within clinically acceptable agreement for implementation at ICC.

TABLE OF CONTENTS

| | |
|--|-----|
| ABSTRACT..... | iii |
| LIST OF TABLES..... | vi |
| LIST OF FIGURES..... | vii |
| 1) INTRODUCTION..... | 1 |
| 2) MATERIALS AND METHODS..... | 5 |
| 2.1) Grid Therapy..... | 5 |
| 2.1.1) Physical Grid Block..... | 5 |
| 2.1.1.1) Commissioning of Physical Block..... | 6 |
| 2.1.1.2) Patient Selection and Prescription..... | 10 |
| 2.1.1.3) Simulation and Treatment Planning..... | 11 |
| 2.1.1.4) Plan Evaluation Metrics..... | 12 |
| 2.1.1.5) Quality Assurance..... | 13 |
| 2.1.2) Virtual Grid using Multi Leaf Collimator..... | 14 |
| 2.1.2.1) Patient Selection and Prescription..... | 14 |
| 2.1.2.2) Simulation and Treatment Planning..... | 14 |
| 2.1.2.3) Plan Evaluation Metrics | 16 |
| 2.1.2.4) Quality Assurance..... | 16 |
| 2.2) Lattice Therapy..... | 17 |
| 2.2.1) Patient Selection and Prescription..... | 17 |
| 2.2.2) Simulation and Contouring..... | 17 |
| 2.2.3) Treatment Planning..... | 21 |
| 2.2.4) Plan Evaluation Metrics..... | 22 |

| | |
|--|----|
| 2.2.5) Quality Assurance..... | 24 |
| 3) RESULTS..... | 25 |
| 3.1) Grid Therapy..... | 25 |
| 3.1.1) Physical Grid Block..... | 25 |
| 3.1.1.1) Dosimetric Characteristics of the Block..... | 25 |
| 3.1.1.2) Treatment Planning and Plan Evaluation Metrics..... | 31 |
| 3.1.1.3) Quality Assurance..... | 34 |
| 3.1.2) Virtual Grid using Multi Leaf Collimator..... | 34 |
| 3.1.2.1) Treatment Planning and Plan Evaluation Metrics..... | 34 |
| 3.1.2.2) Quality Assurance..... | 38 |
| 3.2) Lattice Therapy..... | 38 |
| 3.2.1) Treatment Planning and Plan Evaluation Metrics..... | 38 |
| 3.2.2) Quality Assurance..... | 43 |
| 4) DISCUSSION..... | 44 |
| 5) CONCLUSION..... | 49 |
| REFERENCES..... | 50 |
| CURRICULUM VITAE..... | 55 |

LIST OF TABLES

| | |
|---|----|
| Table 1: Comparison between point doses measured using films and TPS at different depths..... | 28 |
| Table 2: Comparison between grid output factors and open field output factors..... | 30 |
| Table 3: Grid output factors..... | 30 |
| Table 4: Blocked to open area ratio for different field sizes..... | 31 |
| Table 5: Dosimetric parameters for physical block grid plans..... | 33 |
| Table 6: QA for grid plans..... | 34 |
| Table 7: Dosimetric parameters for 3D MLC based SFRT plans..... | 36 |
| Table 8: Doses to the critical structures for 3D MLC based SFRT plans..... | 37 |
| Table 9: Dosimetric parameters for LRT plans..... | 41 |
| Table 10: Doses to the critical structures for LRT plans..... | 42 |

LIST OF FIGURES

| | |
|--|----|
| Figure 1: Grid block by Dot Decimal..... | 5 |
| Figure 2: Set-up of the physical grid block for film measurements..... | 6 |
| Figure 3: Block properties of the grid block..... | 8 |
| Figure 4: Single field grid plan..... | 9 |
| Figure 5: Beam's eye view for a grid treatment field..... | 12 |
| Figure 6: Beam's eye view for a 3D MLC based SFRT plan (GTV<15cm) | 15 |
| Figure 7: Beam's eye view for a 3D MLC based SFRT plan (GTV>15 cm) | 16 |
| Figure 8: Structure template for LRT plans..... | 18 |
| Figure 9: Contouring for LRT plans..... | 19 |
| Figure 10: Volume ratio graph..... | 20 |
| Figure 11: Plan template for LRT plans..... | 21 |
| Figure 12: Objective template for LRT plans..... | 22 |
| Figure 13: Maximum point doses for serial organs | 23 |
| Figure 14: Volumetric objectives for parallel organs..... | 23 |
| Figure 15: Diameter of the hole and center to center spacing..... | 25 |
| Figure 16: Hole diameter measured using RIT..... | 26 |
| Figure 17: Center to center spacing measured using RIT..... | 26 |

| | |
|---|----|
| Figure 18: Vertical and horizontal beam profiles at d_{max} | 27 |
| Figure 19: Vertical and horizontal beam profiles at depth 5cm..... | 28 |
| Figure 20: Comparison of transverse beam profiles for 10 MV beam at d_{max} (A) and 10 cm (B).. | 29 |
| Figure 21: Comparison of radial beam profiles for 10 MV beam at d_{max} (A) and 10 cm (B)..... | 29 |
| Figure 22: Views of isodose distribution for a physical block grid plan..... | 32 |
| Figure 23: Views of isodose distribution for a 3D MLC based SFRT plan..... | 35 |
| Figure 24: Views of isodose distribution for a 3D MLC based SFRT plan..... | 36 |
| Figure 25: Second MU check for a 3D MLC based SFRT plan..... | 38 |
| Figure 26: Views of isodose distribution for a LRT plan..... | 39 |
| Figure 27: Views of isodose distribution showing no bridging between high dose spheres..... | 39 |
| Figure 28: Views of isodose distribution for a LRT plan..... | 40 |
| Figure 29: Views of isodose distribution showing no bridging between high dose spheres..... | 40 |
| Figure 30: QA for a LRT plan showing predicted and portal dose..... | 43 |

1) INTRODUCTION

The most effective non- surgical modality for cancer treatment is radiotherapy (Griffith et al., 2020). In the orthovoltage era, the delivery of therapeutic doses to bulky, deep-seated tumors with a reduction of skin toxicity was achieved by irradiating through a perforated screen called a grid, which produces an array of pencil beams (Mohiuddin et al.,1990). Studies have shown that the normal tissue damage from x rays can be limited if the target volume is divided into discrete sub volumes (Yan et al., 2020), and Alban Köhler first demonstrated the concept of grid over a century ago (Laissue et al., 2012). Grid therapy was abandoned with the advent of Megavoltage treatment units because of the skin sparing effect of a megavoltage beam (Li et al., 2023; Mohiuddin et al.,1990). In 1999, Mohiuddin et al. reported better overall response rates, dramatic relief of severe symptoms, above average local control rates, significant objective regression, and minimal toxicity in treating patients with bulky malignant tumors by using a single-field high dose (10-20 Gy) grid irradiation in conjunction with conventional external beam therapy (>40Gy). This led to renewed interest in grid therapy as a treatment technique. Several other studies have been published about the outcomes of grid therapy, which is considered the original technique to deliver SFRT (Huhn et al., 2006; Peñagaricano et al., 2010; Neuner et al., 2012; Edwards et al., 2015). Since then, improved SFRT methods like lattice radiation therapy with linac (Amendola et al., 2019), helical tomotherapy based grid (Zhang et al., 2016), and Stereotactic Body Radiation Therapy (SBRT) to hypovascularized and hypometabolic tumor segments (Tubin et al., 2019) have arisen.

Therapeutic Ratio (TR) is defined as the ratio of tumor control to the normal tissue complications. Gholami et al. (2016) reported that grid therapy is biologically more effective for radioresistant tumors as the TR of the radioresistant tumor increases with the increase of the

prescribed dose and does not show significant change for radiosensitive tumor. The exact mechanism for grid therapies biological effectiveness is still unknown, but Griffin et al. (2020) sums up the biological mechanisms associated with the response to spatial fractionation as bystander effects, abscopal influence of spatial exposures, vascular effects, and oxygen availability. Bystander effects are signal mediated effects in non-irradiated cells from nearby irradiated cells (Asur et al., 2015). Abscopal effect is the tumor regression induced by radiotherapy in lesions distant from the target site as the antitumor immunity is stimulated by the dying tumor cells that release tumor associated antigens (Massacesi et al., 2020). The immunogenic cell death might be triggered more efficiently if central hypoxic tumor segment gets high dose of radiation while sparing lymphocytes at the tumor periphery (Massacesi et al., 2020). Tubin et al. delivered SBRT to the hypoxic segment of unresectable bulky tumors. Abscopal and bystander effects were triggered, and this treatment showed 96% overall response rate. Other biological effect that happens following SFRT with grid technique is the enhanced reoxygenation of the tumor which causes the regression of the tumor mass clinically as tumor is treated with chemoradiation following the grid dose (Huhn et al., 2006).

An ideal peak to valley configuration should be such that the peak dose should be sufficiently high to induce immunogenic response and valley dose regions sufficiently low to preserve the lymphatic cells, tumor microvasculature and perfusion to allow cytokines circulation (Wu et al., 2020). Also, this technique leads to increased cytokine production which results in broad systemic effects (Peñagaricano et al., 2010). The dying tumor cells release the tumor antigens which interact with the immunostimulatory cytokines resulting in antitumor immune response (Pokhrel et al., 2022). The killing of endothelial cells inside the tumor can lead to an avalanche of tumor cell death (Yan et al., 2020). For induction of endothelial apoptosis to achieve

treatment efficacy, a dose greater than 12 Gy is required; for cytokine release associated with bystander effects, doses greater than 10 Gy is required (Nobah et al. 2015). Zwicker et al. (2004) used a linear quadratic model to evaluate radiobiological properties of grid irradiation and concluded the significant therapeutic advantage of using a single dose of grid therapy over open radiotherapy in sparing normal tissues.

Evaluation of the dosimetric characteristics of the different grid blocks has been previously published which helps in the safe and accurate standardization of grid block clinical implementation (Meigooni et al., 2006; Buckey et al., 2010; Nobah et al., 2015; Zhang et al., 2020). With modern Linacs, MLC can also be used to create grid equivalent dosimetry. There are several advantages to this method such as not needing to lift heavy physical blocks as well as the flexibility to change hole size and separation during planning (Yan et al., 2019). Disadvantages of the technique include the fact that using MLCs to form the same hole size as a physical block can cause dose spillage to the shielded area due to interleaf leakage. Also, MLC based grid can increase Monitor Units (MU) by over 500% versus using a physical block, resulting in longer patient treatment times (Buckey et al., 2010). Pokhrel et al. published a 3D MLC based SFRT planning technique that uses lower MUs. Part of the challenge of treating deep seated tumors with conventional grid therapy is keeping doses sufficiently low to the adjacent normal tissue. New SFRT techniques utilizing Volumetric Arc Therapy (VMAT) have been developed to reduce the dose to normal tissue while ensuring a high dose to the tumor. These techniques are generally known as LRT (Yan et al., 2019). This therapy is delivered by creating multiple high dose spheres called vertices within the tumor while keeping lower dose in the tumor periphery to avoid dose to the critical structures.

The scope of the project is to implement SFRT techniques at the ICC for a Varian Truebeam linear accelerator. This technique would help in achieving high biological effective dose for the treatment of bulky tumors while sparing nearby OARs. The clinical implementation of this technique requires the development of the treatment planning methods along with quality assurance. For grid therapy, the commissioning of the physical block was performed (beam profiles, output factor, isodose distribution and percentage depth dose of radiation field). Dosimetric verification for a 10 MV beam was performed using Gafchromic EBT3 film. Dosimetry metrics that decide plan acceptability were also established.

2) MATERIALS AND METHODS

2.1) GRID therapy

2.1.1) Physical grid block

The grid block used was developed by Dot Decimal (Sanford, FL; Model # 5202) and is shown in Figure 1. It produces a non-uniform dose distribution with high and low dose areas through a perforated screen. The dimensions of the brass block are 17cm x 18cm x 7.62 cm and weighs 15.8 kg. Grid holes are designed to match the divergence of the linear accelerator. Hole diameter at the isocenter is 1.43 cm and the grid spacing is 2.11 cm. The maximum field size that the grid block can treat is 25 cm x 25 cm at isocenter. Grid block is mounted to a tray that slides into the linac accessory mount such that the custom block tray distance from source is 65.4 cm.

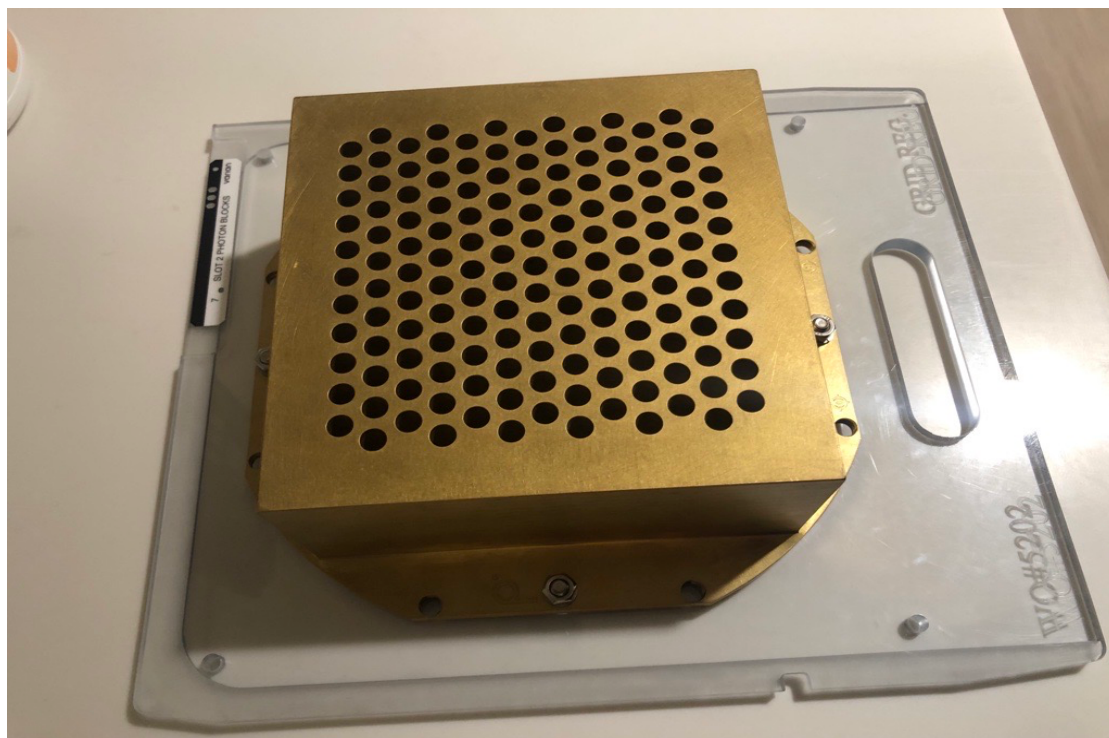


Figure 1: Grid block by Dot Decimal.

2.1.1.1) Commissioning of Physical Block

Grid block commissioning consisted of measuring the dimensions of the grid block, transmission factor, inline and crossline profiles at different depths of solid water and determining grid output factors. Dosimetric comparisons between the measured data and Eclipse Treatment Planning Systems (TPS) computed results were made for treatment plans and analyzed for agreement within 3% uncertainty.



Figure 2: Set-up of the physical grid block for film measurements.

A Varian Truebeam linear accelerator was used to perform all the measurements. All grid-based treatment plans were created in Eclipse TPS (Version 16.1) using a 10 MV photon beam. Gafchromic EBT3 film (Ashland, NJ) was calibrated using 10MV photons with a dose range of 0 - 20 Gy using 5 x 5 cm² open field at depth of maximum dose (dmax) in solid water phantom material at 100 cm SAD. The setup of the physical grid block for film measurement is shown in Figure 2. The accuracy of the calibration was tested by irradiating the film with the known dose and analyzing it with the Radiological Imaging Technology (RIT) software (Version 6.11).

Grid dimensions and treatment planning system commissioning

The grid hole diameter and grid spacing was measured by irradiating the Gafchromic EBT3 film positioned at isocenter. Grid dimensions were verified by scanning the film using an EPSON 10000 XL scanner, measuring in Eclipse TPS (Version 16.1) and analyzing it with the RIT.

To introduce the physical grid block in the Eclipse TPS, a single field treatment plan was created and sent to the vendor to generate a library of block files. Each block file was only able to be used on an individual patient basis. The block files script received from the vendor were then modified to fit the individual treatment plan as needed and imported into Eclipse TPS.

Grid block parameters were inserted into the Eclipse TPS. A photon custom coding label was attached to the right corner of the tray and this same photon custom code was inserted in the block properties in Eclipse, allowing the Truebeam to recognize the grid block when it is attached to the accessory mount. Other parameters related to the grid block like material code, block transmission, slot ID, source-to-slot distance, tray ID, custom code, and tray transmission are shown in Figure 3.

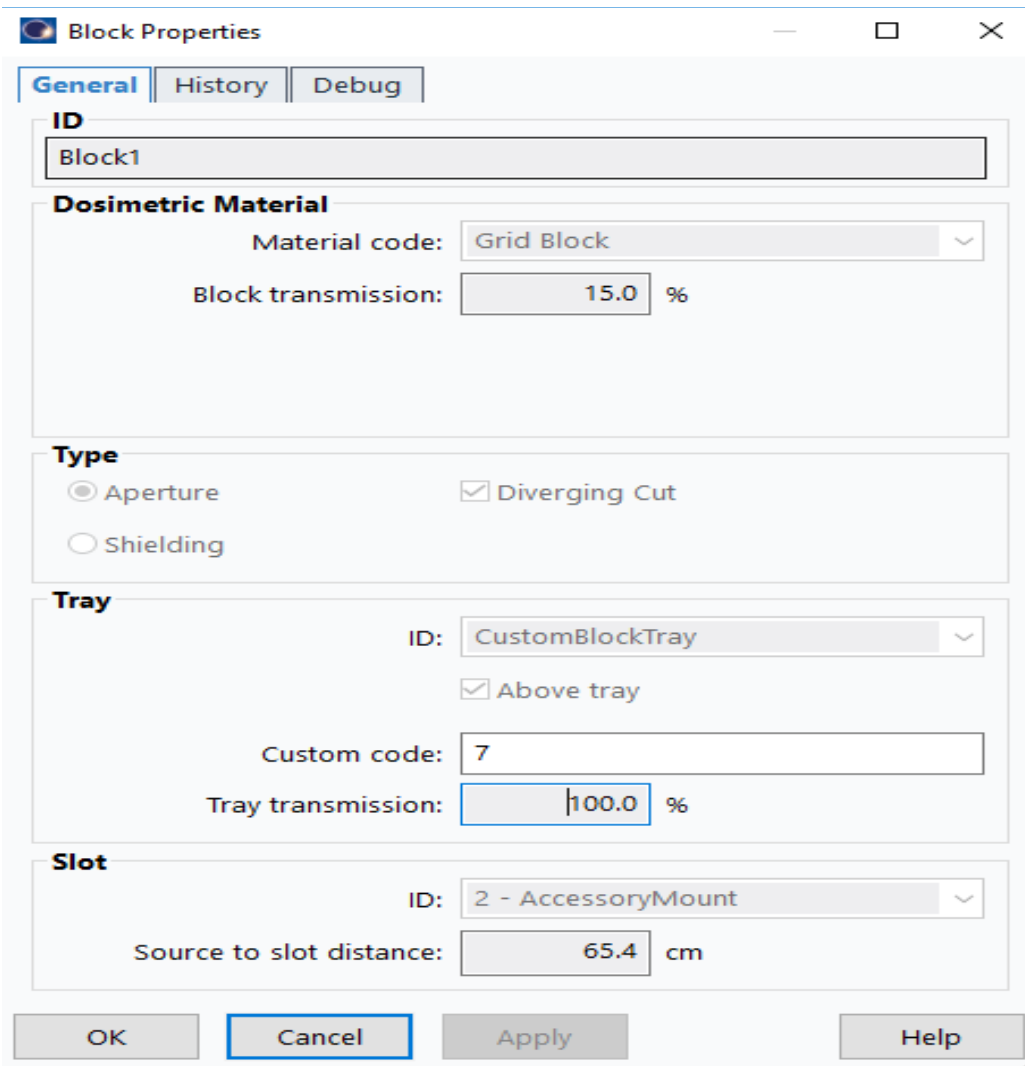


Figure 3: Block properties of the grid block.

Transmission factor of the Grid block

A solid water phantom was scanned using GE CT scanner. To get the Eclipse TPS generated dose profiles, a single field plan was created using Acuros algorithm for 10 MV photon beam, 18x18 cm² field size, and 400 MU. The resulting dose is shown in Figure 4. The coronal dose plane was then exported from the Eclipse TPS and compared with the measured film dose profiles.

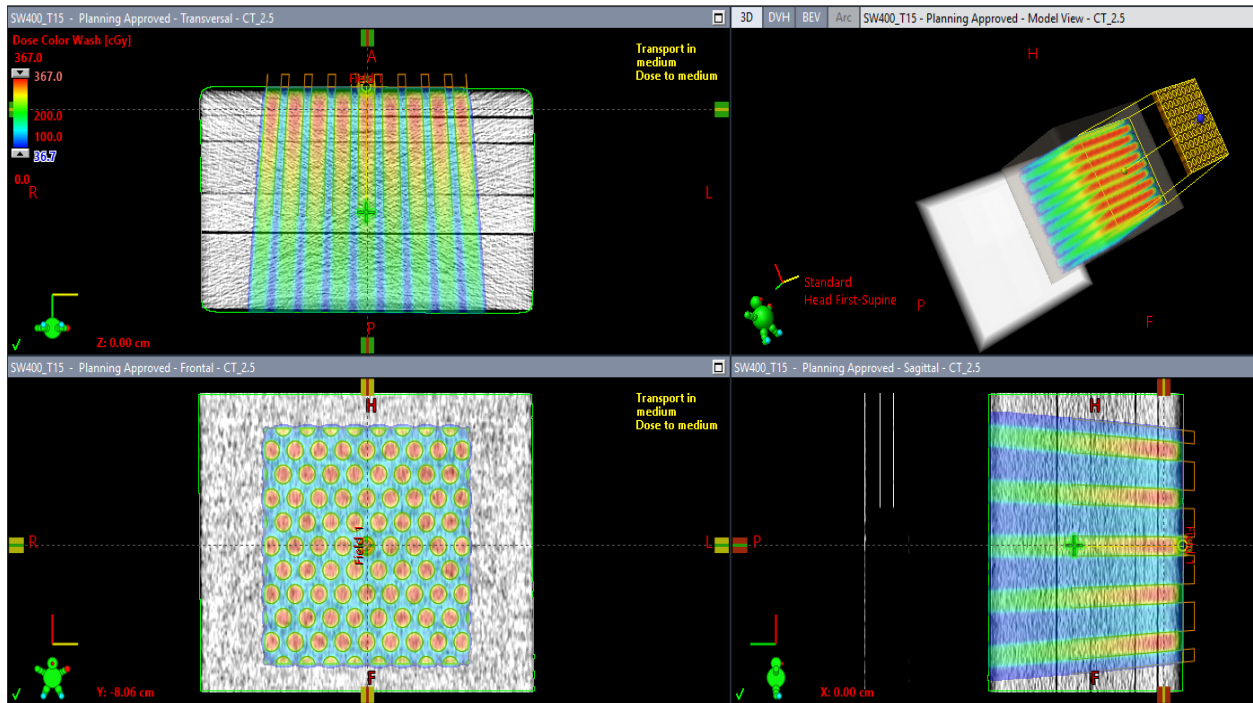


Figure 4: Single field grid plan.

Gafchromic EBT3 film was placed at d_{max} and irradiated using the same plan geometry. After 24 hours, the film was scanned using the EPSON 10000 XL scanner and analyzed using RIT. The dose plane exported from the Eclipse TPS was registered with the film and the dose profiles were compared.

The transmission factor of the grid block is defined as the ratio of the dose measured under blocked region to that measured without block in water for the same MU. The block transmission was found by setting up different values in the block properties of the Eclipse TPS and then by comparing it with the film measurements.

Profile measurements

Gafchromic EBT3 film was placed in solid water and irradiated using a 10 MV photon beam at depths of 2.3cm (d_{max}), 5 cm, 10 cm, 15 cm in a plane perpendicular to the central beam

axis. After 24 hours post-irradiation, the film was scanned using an EPSON 10000XL scanner. The in-line and crossline beam profiles were obtained using RIT software by applying the film calibration file specific to this batch of films. The film profiles were compared to the dose planes from the Eclipse TPS at the same depths.

Dosimetric measurements

Film dosimetry was used to measure blocked to open area ratio using the following parameters: 10 MV beam, 300MU, 5x5, 10x10, 15x15, 20x20, 25x25 cm² fields at dmax using SAD set up. Output factors of the grid were measured using the PTW microdiamond detector placed at dmax in the sun nuclear 1D water tank (model number 1233) for the following parameters: 10 MV, 100 MU, 3 x 3 cm² to 25 x 25 cm², and 100cm SSD. Scanning system was carefully aligned to maintain the microdiamond detector at the center of the beam profile at all depths. The detector measurements were normalized to an open 10x10 cm² field with the detector placed at dmax. Point dose measurements at the central hole for dmax, 5 cm, 10 cm, and 15 cm depth were measured using film dosimetry and compared it with the point doses in the isodose plan created in Eclipse TPS.

2.1.1.2) Patient Selection and Prescription

Good candidates for SFRT generally fit the following criteria: patients with bulky tumors (≥ 5 cm); patients with radioresistant tumors; patients who require rapid symptom relief; and patients with superficial tumors where the chosen beam angle can entirely avoid OARs (e.g., breast or extremities). SFRT can also be used for inducing immunostimulatory effect or reducing tumor volume before treating the patient with conventional fractionation (Grams et al., 2023).

Grid therapy should be a single fraction from 10-20 Gy prescribed at the d_{max} for a given beam size if tumor is shallowly seated (<3cm deep) and prescribed at the tumor center depth if tumor is deeply seated (>3cm) (Zhang et al., 2020). Treatment plans were created using 15 Gy prescribed at the d_{max} for a 10 MV beam.

2.1.1.3) Simulation and Treatment Planning

Conventionally, the treatment planning for grid therapy was performed without CT simulations and used a clinical set up to perform MU hand calculations. However, the clinical set up technique does not provide 3D dose distribution in the patient. For this project, prior CT simulation scans were used to generate five treatment plans using grid technique. 3D CT images were taken using GE Optima 16 slice CT scanner with 512 x 512 pixels (2.5 mm slice thickness). Treatment isocenter was placed at 100 cm SSD and the beam's central axis was aligned with the center of the target. Our clinic plans to use 10MV for grid treatments due to concern of neutron creation over 10 MV. The dose was prescribed to the d_{max} , which is 2.3cm for a 10 MV photon beam. The reference point was placed at d_{max} , and prescription dose was normalized to the reference point in the Eclipse TPS. The reference point was placed at the center of an open aperture along the central axis making sure that the reference point is under the open portion of the field. Collimator angle and couch rotation were optimized to minimize normal tissues in the field and maximize tumor exposure.

Planning Target Volume (PTV) for grid therapy was generated by subtracting an inner margin of 5mm from the physician drawn Gross Tumor Volume (GTV) (increased to 1 cm in case there is an uncertainty about the location of the OAR) (Grams et al., 2023). The jaws and MLC were fit to the PTV, and MLCs were moved to provide extra blocking of the normal tissue that

may be in the field. The beam's eye view of the beam delivered using Eclipse TPS for physical grid block is shown in Figure 5.

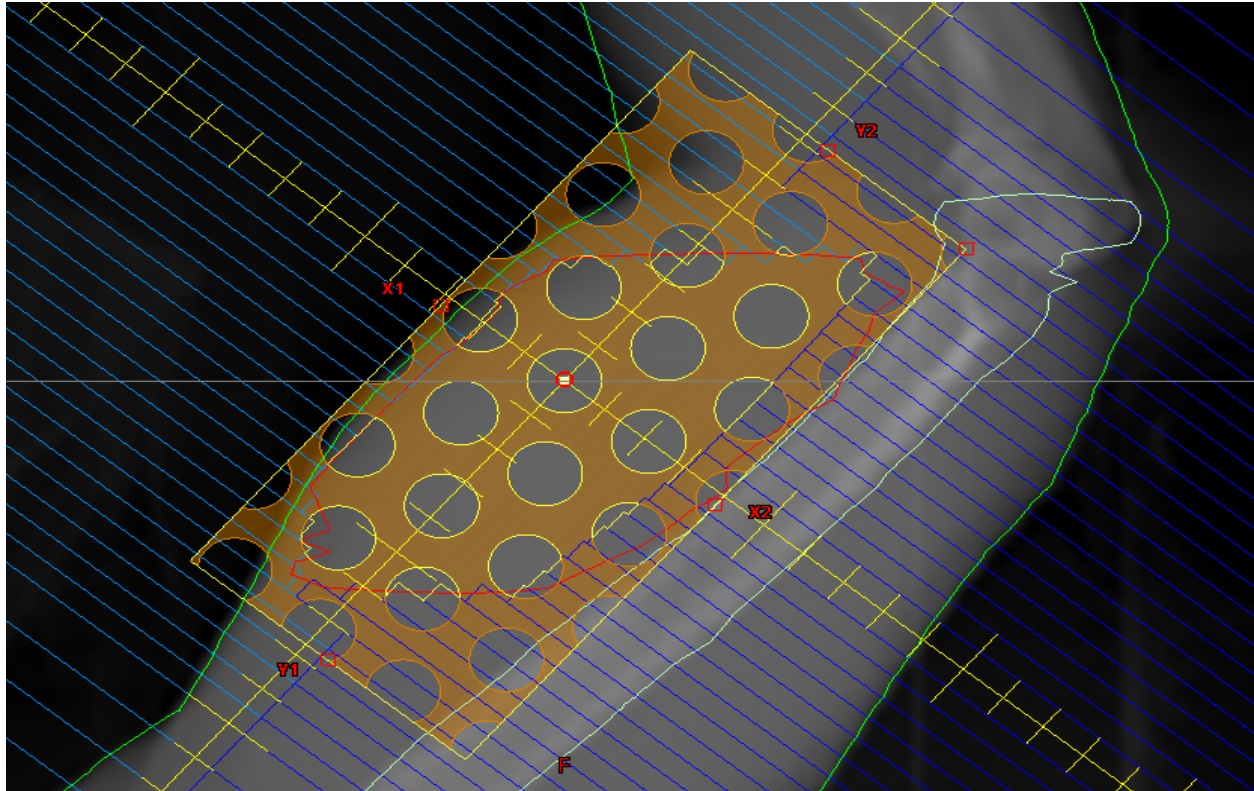


Figure 5: Beam's eye view for a grid treatment field. Humerus (light green color contour) of the right arm with 1 cm margin was shielded using MLC from the grid field and medial portion of the GTV (red color contour) cannot be treated with field. The SSD was set to 100 cm and a reference point was placed along the central axis at d_{max} in the middle of an open aperture and prescription dose was normalized to the reference point.

2.1.1.4) Plan Evaluation Metrics

Due to the intentional non uniform dose distribution of the grid, conventional dose constraints to the PTV are not applicable. Instead, the Equivalent Uniform Dose (EUD) should be reported to describe the grid dose. The EUD for tumors is the Biologically Equivalent Dose (BED)

if homogeneously given to the tumor can cause same cell kill as the non-uniform dose distribution. The approximation equation to calculate EUD for a 3D tumor treated with the grid therapy with nominal dose ≥ 5 Gy is

$$\text{EUD} = 2.47 + 0.089 \times D_{\text{nominal}} \quad (\text{Zhang et al., 2020})$$

The physics working group also recommends reporting the dose covering 90%, 50%, 20%, 10% and 5% of the target and Peak to Valley Dose Ratio (PVDR) (Zhang et al., 2020). Also, the beam energy selected for the grid treatment let 50% isodose line to extend to the farthest part of the target making sure that the exit dose into any critical structure is acceptable (Grams et al., 2023).

2.1.1.5) Quality Assurance

Patient specific QA using portal dosimetry was not required for 3D MLC based SFRT plans. To verify the MU for the plans using hand calculations, verification plans were created for the test plans using solid water phantom with the gantry angle set to zero. The effective size of the field with MLC blocking was obtained from the properties of the field in the Eclipse TPS. The output factor for the effective field was interpolated from the output factor table. The MU was calculated by dividing the nominal dose by the product of output factor and inverse square factor.

$$\text{MU} = \frac{\text{Dose}_{(\text{nominal})(\text{cGy})}}{\text{Output factor}_{(\text{dmax})(\frac{\text{cGy}}{\text{MU}})} \times \frac{(\text{SSD})^2}{(\text{SSD}+\text{dmax})^2}}$$

If physician decides to prescribe to a depth other than dmax, the grid output factor at that depth must be measured or calculated.

2.1.2) Virtual GRID using MLC

Pokhrel et al. (2022) developed a CBCT guided 3D conformal MLC-based SFRT technique for effectively treating bulky tumors (≥ 8 cm). This technique allows the dose to be escalated for deep lesions to debulk unresectable large tumors which is a good option for neoadjuvant treatment.

2.1.2.1) Patient selection and Prescription

Pokhrel et al. (2022) reported fast treatment of 50 extracranial patients with bulky tumors with 3D MLC based SFRT technique. The treatment sites reported were extremities, H&N, liver, chest tumors, abdominal/pelvis, adrenal, neglected breast, and paraspinal masses. The patients who were selected for this technique had GTV ≥ 8 cm and prescription dose was 15 Gy.

2.1.2.2) Simulation and Treatment Planning

Prior CT simulation scans were used to generate five treatment plans using 3D MLC based SFRT technique in the Eclipse TPS. 3D CT scans were taken using a GE Optima 16 slice CT scanner with 512 x 512 pixels (2.5 mm slice thickness). 4D CT scans were acquired for the patients with moving targets. If the motion was less than 5mm, no motion management was required but if the motion was greater than 5mm, motion management using breath hold or abdominal compression was implemented.

To create 3D MLC SFRT plans, 6 coplanar crossfire treatment fields with gantry angles at 60° equal spacing and collimator set to 90° was used. For each treatment field, either 6 MV or 10 MV photon beams were chosen. The gantry angles used were 30° , 90° , 150° , 210° , 270° , 330° . Millennium 120 MLC leaves were used to generate holes of 1cm diameter and 2 cm spacing at isocenter. As shown in the Figure 6, the MLC aperture was fit to the GTV drawn by the physician, two MLCs (5mm each) were opened at the isocenter, two MLCs were closed on left and right side

of the isocenter, and this pattern was manually repeated to cover the GTV for each gantry angle. To minimize the MLC interleaf leakage, either bank A or bank B of MLC was positioned outside the jaws if tumor was less than 15 cm as shown in Figure 6 but if the tumor was greater than 15cm, the MLCs were closed at different levels as shown in Figure 7. The beam weighting and energy for each treatment field were modified based on the depth of the tumor and proximity of critical structures to achieve better coverage of the target and limit OAR maximum doses as per American Association of Physicists in Medicine (AAPM) Task Group (TG) 101.

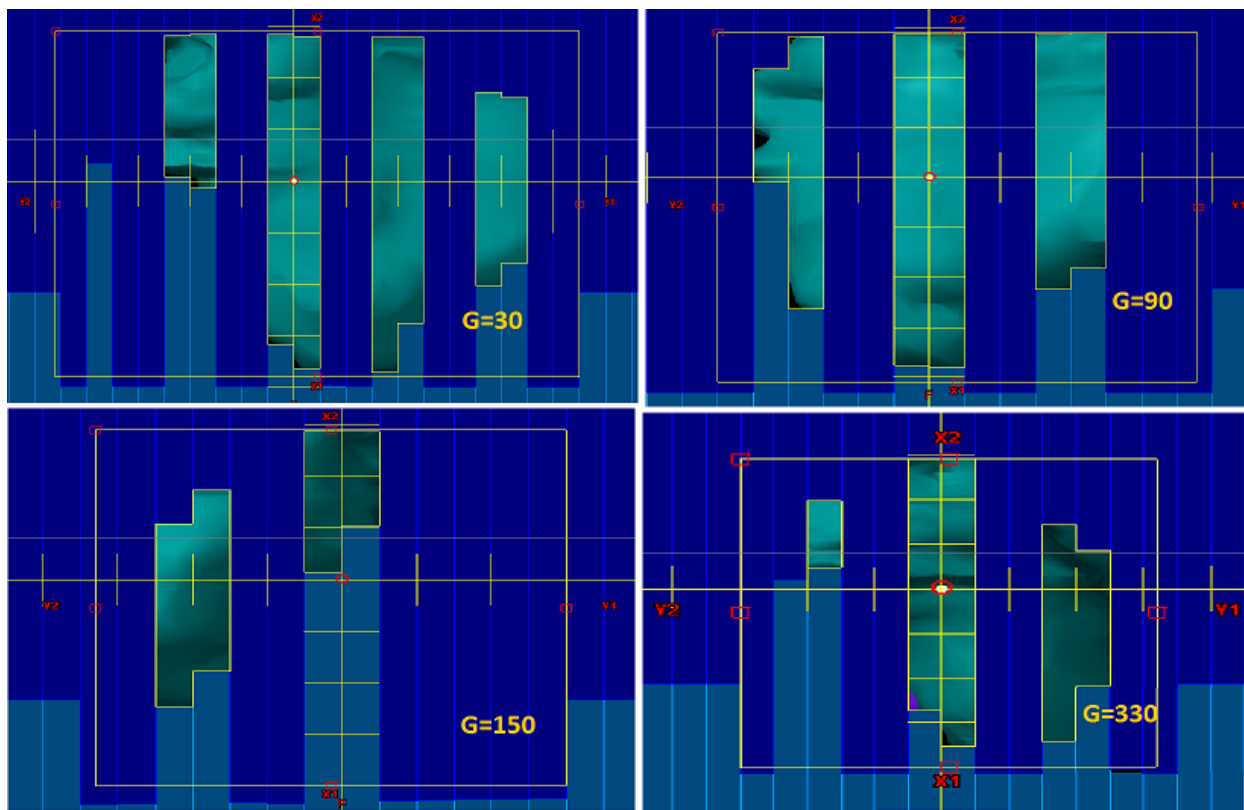


Figure 6: Beam's eye view for a 3D MLC based SFRT plan (GTV < 15cm). Plan was created for a patient with left thigh liposarcoma (GTV 114.92 cc, length 5cm). 4 out of 6 gantry angles were used. The 270 degree was not used due to large patient separation and 210 was not used to minimize dose to femur. MLCs were modified to reduce the dose to the critical structures (femur and genitalia).

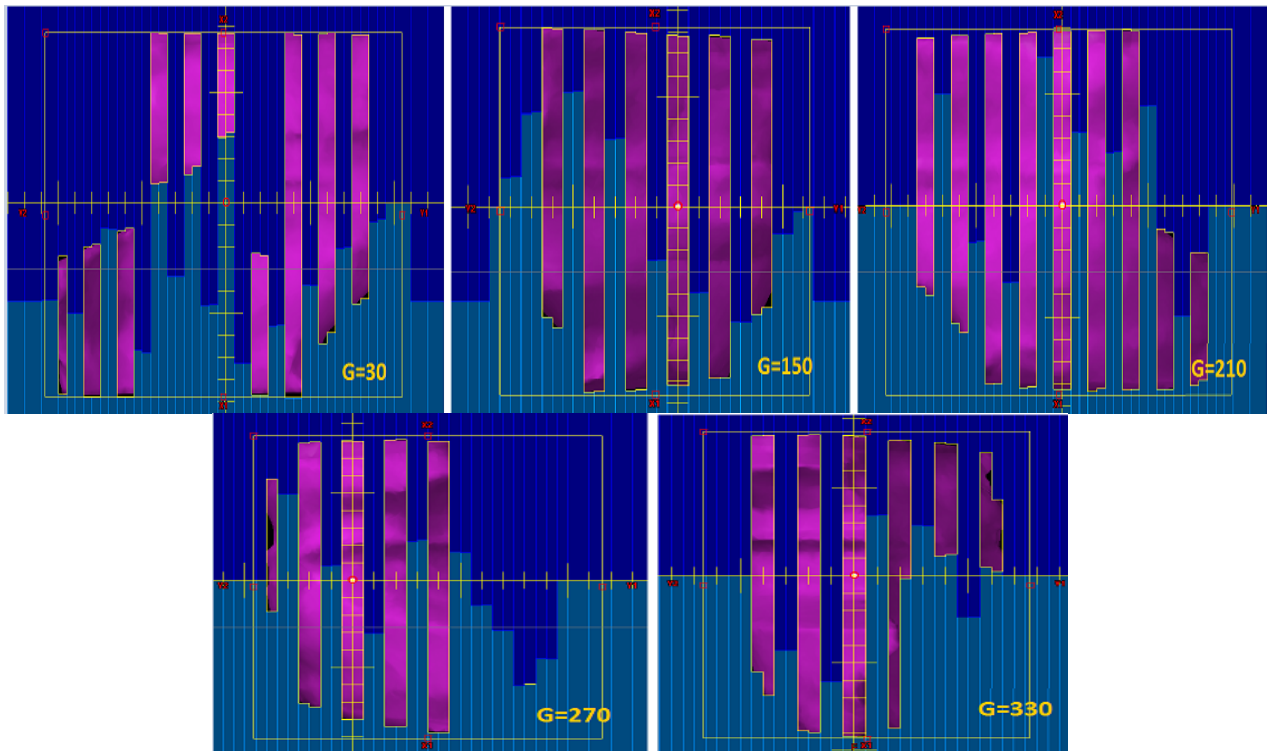


Figure 7: Beam's eye view for a 3D MLC based SFRT plan (GTV > 15 cm). Plan was created for a patient with right buttock leiomyosarcoma (GTV 2598 cc, length 17cm). 5 out of 6 gantry angles were used, and MLCs were modified to reduce the dose to the critical structures (bowel and femur).

2.1.2.3) Plan Evaluation Metrics

The dosimetric parameters that decide the acceptability of the 3D MLC based SFRT plan is PVDR, mean GTV dose, GTV (in percentage) receiving 7.5 Gy, and maximum dose to the critical structures as per AAPM TG 101.

2.1.2.4) Quality Assurance

The patient specific QA using portal dosimetry was not required for 3D MLC based SFRT plans. The calculation of MU per treatment field for physics second check was performed using a third-party software Clear Check (Radformation, Inc., New York, NY).

2.2) Lattice therapy

Lattice therapy uses VMAT to generate an array of high dose vertices within the tumor while reducing peripheral dose. The desired dose gradients and normal tissue sparing can be achieved as LRT technique provides flexibility in placing high dose spheres within tumor.

2.2.1) Patient Selection and Prescription

Selected patients for LRT are those with deeper tumors in the abdomen, thorax, pelvis, or head and neck which are surrounded by OARs that cannot be spared by grid technique. These critical organs can be spared by the dose optimization capability of VMAT which make it an efficient technique to be used for any location in the body.

Wu et al. (2020) reported the prescription dose of 2.4 to 20 Gy peak dose per fraction delivered in 1 to 5 fractions using a high dose sphere vertex diameter of 0.5 - 1.5cm distributed within GTV with center-to-center separation of 2 – 5 cm. Kavanaugh et al. (2022) reported the achieved dosimetric characteristics specific to LRT technique described by Wu et al. (2020) and OAR constraint were used from AAPM TG-101. Duriseti et al. (2021) described the LRT technique that used VMAT to deliver 20 Gy in 5 fractions with simultaneous integrated boost of 66.70 Gy. This prescription was used in this project to create five test treatment plans. In this study, the patients with minimum size of 4.5 cm (any histology) for the solid tumor were selected as 4.5 cm size allowed the placement of 1 high dose sphere inside the 1cm reduction of the tumor.

2.2.2) Simulation and Contouring

CT Images of patients who were previously treated at our institution were used to create the LRT plans. The new structure template for the LRT technique shown in Figure 8 was created in the Templates and Clinical Protocols workspace of the Eclipse TPS.

Structure Templates

| ID | Volume Type | Structure Code | Color and Style |
|--------------|-------------|----------------|------------------|
| PTV_6670 | PTV | PTV High Risk | RGB204 0 0 |
| PTV_2000 | PTV | PTV High Risk | RGB119 0255 |
| GTV_2000-1cm | GTV | GTV Primary | RGB128 0128 |
| GTV_2000 | GTV | GTV Primary | RGB 0160160 |
| NS_Ring_20 | Control | Control Region | RGB116 27 71 |
| DR_1.5 | Control | Control Region | RGB106168 79 |
| PTV_Avoid | Control | Control Region | Segment - Magent |
| PTV_Control | Control | Control Region | RGB224102102 |

Figure 8: Structure template for LRT plans.

The GTV_2000 drawn by the physician includes all visually identifiable gross disease was expanded by 0.5 to 1 cm to create the PTV_2000. The 1 cm retraction of the GTV was generated for GTV less than 2000 cc (GTV_2000-1cm) and 1.5 cm retraction of the GTV was generated for GTV greater than 2000 cc (GTV_2000-1.5cm). In the center of the PTV_2000, the viewing plane indicators were matched to the grid intersection in all three planes. To generate PTV_6670, the 3 cm grid was turned on in the contouring workspace and high dose vertices were placed inside GTV_2000-1.5cm at the alternating grid intersections using a 1.5 cm brush (3D) to create 6 cm center-to-center spacing. The 1.5 cm PTV_Avoid vertices were alternated with PTV_6670 high dose spheres so that distance between them is 3cm as shown in Figure 9. The process of placing PTV_6670 and PTV_Avoid every 3 cm in superior and inferior direction was repeated.

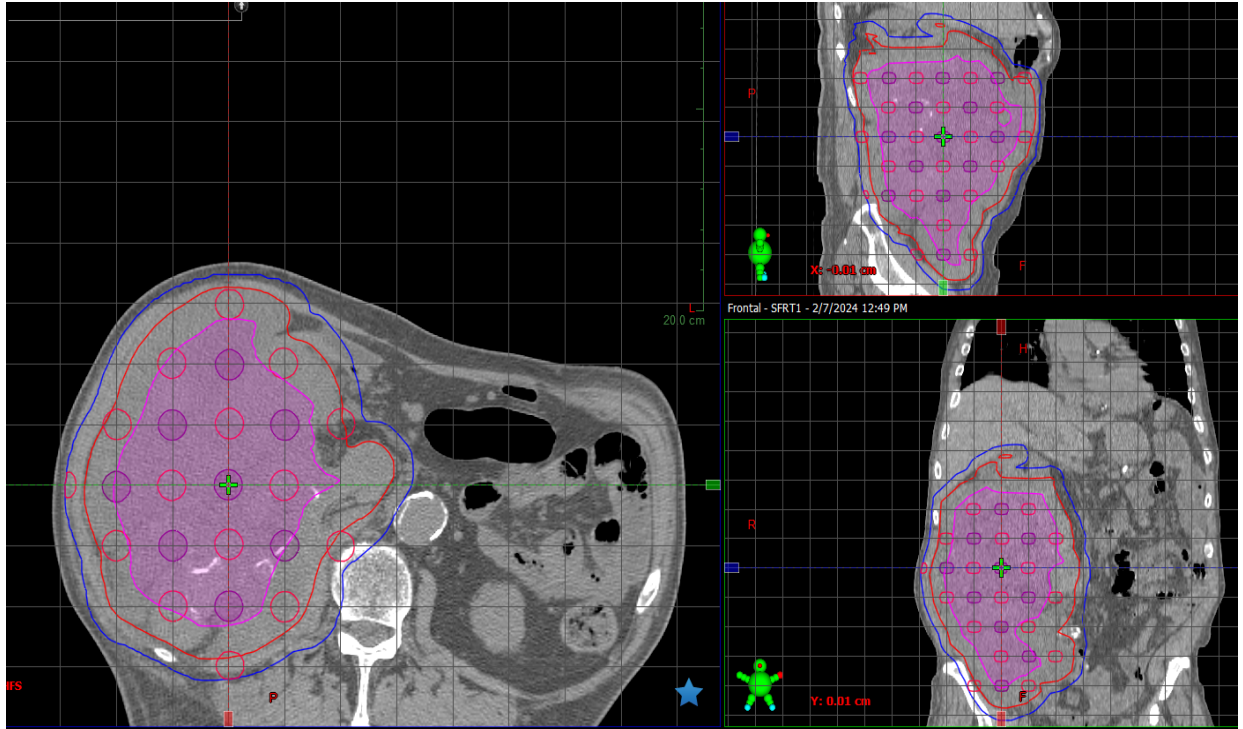


Figure 9: Contouring for LRT plans. Axial, sagittal, and coronal planes showing PTV_6670 high dose spheres contoured in purple color and PTV_Avoid spheres that are placed alternately at the grid intersections between the high dose spheres for a patient with liposarcoma of the right retroperitoneum (GTV 3445 cc). PTV_2000 (blue), GTV_2000 (red), GTV- 1.5 cm (pink) are also shown.

PTV_6670 high dose spheres were modified by applying axial rotation or sup-inf translation to maximize number of full spheres inside the GTV_2000 - 1.5 cm. The modifications applied to PTV_Avoid was identical to PTV_6670 so that the global geometric structure was maintained. To achieve identical modifications for both the structures, the translations and rotations were first applied to PTV_6670. PTV_6670 was then copied on to PTV_Avoid structure and translated 3cm within the axial plane so that those spheres were evenly placed within the high dose spheres. All spheres of PTV_Avoid that extended 50 % outside PTV_2000 and all spheres of PTV_6670 that extended 50% outside GTV – 1.5 cm were removed. To achieve the objective for critical structures, the PTV_6670 spheres were shifted by up to 3mm or individual spheres

were removed. The graph shown in Figure 10 from Kavanaugh et al. (2022) was used as a reference to decide the number of high dose spheres for PTV_6670 structure for all the LRT plans.

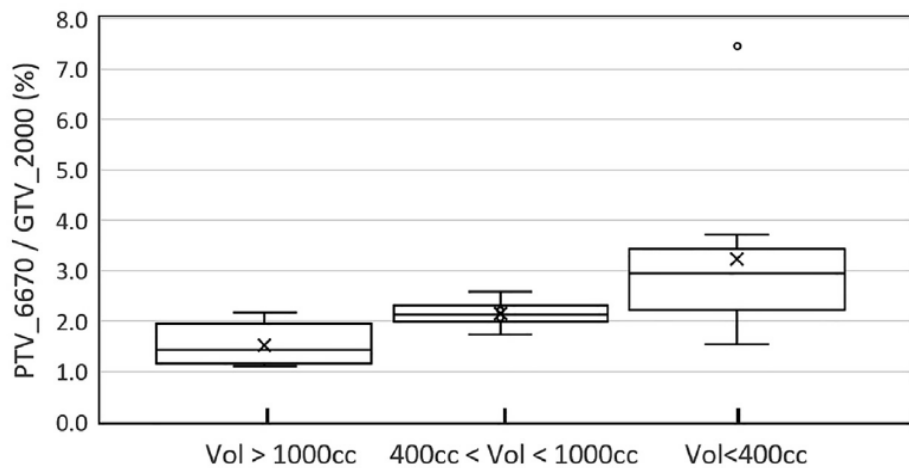


Figure 10: Volume ratio graph. The ratio of PTV_6670 and GTV_2000 (in %) as a function of GTV_2000 (Kavanaugh et al., 2022).

The other dose optimization structure called PTV_Control was created by cropping PTV_6670 with 8mm margin from PTV_2000 and the structure DR_1.5 was created by cropping PTV_6670 from PTV_6670 + 1.5cm. NS_Ring_20 structure was created by cropping PTV_2000 with 1cm margin from body structure. The planning OAR volumes were created for the organs that are difficult to assess on the CBCT and can displace from their original position (such as rectum, bowel, esophagus, and pulmonary vessels) by using a 5mm expansion from the OAR (Kavanaugh et al., 2022).

2.2.3) Treatment Planning

All plans were generated for Varian Truebeam with standard Millennium 120 MLC using a Varian Eclipse TPS and Acuros algorithm for dose calculation. The plan template was created in the Templates and Clinical Protocol workspace in Eclipse TPS as shown in Figure 11. PTV_6670 was used as planning target for the plan and prescribed a total dose of 66.7 Gy (13.34 Gy per fraction). The isocenter was set to be in the center of the PTV_2000. The LRT plans were created using either 6MV or 10 MV flattening filter free beams depending on the treatment site, full or partial arcs (2 to 4) with up to 10 degrees couch kicks depending on the location of the tumor and couch clearance available, collimator rotation of 15 to 90 degrees, and jaw tracking.

| Field ID | Technique | Machine/Energy | Field Weig... | Scale | Gantry Rtn [deg] | Coll Rtn [deg] | Couch Rtn [deg] | Field X [cm] | Field Y [cm] | X [cm] | Y [cm] | Z [cm] | Calculated SSD [cm] |
|----------|-------------------|--------------------|---------------|------------|------------------|----------------|-----------------|--------------|--------------|--------|--------|--------|---------------------|
| Field 1 | SRS Arc Therapy-I | TrueBeam - 10X-FFF | 1.000 | Varian IEC | 180.1 CW 179.9 | 25.0 | 0.0 | 15.0 | 15.0 | 0.00 | 0.00 | 0.00 | 85.9 |
| Field 2 | SRS Arc Therapy-I | TrueBeam - 10X-FFF | 1.000 | Varian IEC | 179.9 CCW 180.1 | 335.0 | 0.0 | 15.0 | 15.0 | 0.00 | 0.00 | 0.00 | 85.9 |
| Field 3 | SRS Arc Therapy-I | TrueBeam - 10X-FFF | 1.000 | Varian IEC | 180.1 CW 179.9 | 45.0 | 10.0 | 15.0 | 15.0 | 0.00 | 0.00 | 0.00 | 85.9 |
| Field 4 | SRS Arc Therapy-I | TrueBeam - 10X-FFF | 1.000 | Varian IEC | 179.9 CCW 180.1 | 315.0 | 350.0 | 15.0 | 15.0 | 0.00 | 0.00 | 0.00 | 85.9 |

Figure 11: Plan template for LRT plans.

The objective template for the LRT plans in the optimization workspace was created as a starting point and modified to achieve the clinical goals during optimization as shown in Figure 12. A manual normal tissue objective was set for rapid dose fall off with start dose of 100%, end dose of 30%, and distance from target border of 0.3 cm. The OAR objectives were added as needed after starting optimization as per AAPM TG 101.

| | | | | |
|---------------|--------|-------|------|-----|
| PTV_2000 | 5033.2 | | | |
| Upper | 0.0 | 0.0 | 7400 | 60 |
| Lower | 5033.2 | 100.0 | 2050 | 100 |
| PTV_6670 SFRT | 63.9 | | | |
| Upper | 0.0 | 0.0 | 7400 | 60 |
| Lower | 63.9 | 100.0 | 6760 | 90 |
| PTV_AVOID | 125.1 | | | |
| Upper | 0.0 | 0.0 | 3000 | 50 |
| Lower | 125.1 | 100.0 | 2000 | 70 |
| NS_Ring | 1088.1 | | | |
| Upper | 0.0 | 0.0 | 2300 | 50 |
| PTV_Control | 4168.3 | | | |
| Upper | 0.0 | 0.0 | 5000 | 50 |

Figure 12: Objective template for LRT plans.

2.2.4) Plan Evaluation Metrics

The SFRT clinical protocol was created following AAPM TG-101 in Templates and Clinical Protocols workspace in the Eclipse TPS. The serial organs followed maximum point dose constraint as shown in Figure 13 and the parallel organs followed volumetric objectives as shown in Figure 14. The recommended evaluation parameters were PTV_2000 conformity index, dose gradients within the GTV_2000, ratio of mean doses of PTV_6670 and PTV_Avoid structures (DR), and ratio of median dose and standard deviation dose within the 1.5 cm ring outside the PTV_6670 spheres (DR_1.5) (Kavanaugh et al., 2022). The EUD ($a = -10$) for GTV_2000 and ratio of prescription dose and mean dose (95%-100%) for GTV - 1.5cm as recommended by Wu et al. (2020) were also investigated.

Prescription Objectives

| Primary | Plan | Prescription Objectives | | | Fraction Dose [c... | Total Dose [c... | Add | |
|-------------------------------------|----------|-------------------------|--------------|------|----------------------|------------------|--------|--------|
| <input checked="" type="checkbox"/> | SFRT Anu | PTV_6670 | At least | 95.0 | % receives more than | 1334.0 | 6670.0 | Remove |
| <input type="checkbox"/> | SFRT Anu | PTV_2000 | At least | 95.0 | % receives more than | 400.0 | 2000.0 | Remove |
| <input type="checkbox"/> | SFRT Anu | PTV_Av... | Mean dose | | is less than | 460.0 | 2300.0 | Remove |
| <input type="checkbox"/> | SFRT Anu | Esophag... | Maximum dose | | is less than | 600.0 | 3000.0 | Remove |
| <input type="checkbox"/> | SFRT Anu | Spinal C... | Maximum dose | | is less than | 560.0 | 2800.0 | Remove |
| <input type="checkbox"/> | SFRT Anu | Brachial ... | Maximum dose | | is less than | 640.0 | 3200.0 | Remove |
| <input type="checkbox"/> | SFRT Anu | Heart | Maximum dose | | is less than | 760.0 | 3800.0 | Remove |
| <input type="checkbox"/> | SFRT Anu | Stomach | Maximum dose | | is less than | 700.0 | 3500.0 | Remove |
| <input type="checkbox"/> | SFRT Anu | Small B... | Maximum dose | | is less than | 600.0 | 3000.0 | Remove |
| <input type="checkbox"/> | SFRT Anu | Large B... | Maximum dose | | is less than | 800.0 | 4000.0 | Remove |
| <input type="checkbox"/> | SFRT Anu | Rectum | Maximum dose | | is less than | 1100.0 | 5500.0 | Remove |
| <input type="checkbox"/> | SFRT Anu | Bladder | Maximum dose | | is less than | 700.0 | 3500.0 | Remove |
| <input type="checkbox"/> | SFRT Anu | Optics | Maximum dose | | is less than | 500.0 | 2500.0 | Remove |
| <input type="checkbox"/> | SFRT Anu | Cochlea | Maximum dose | | is less than | 440.0 | 2200.0 | Remove |
| <input type="checkbox"/> | SFRT Anu | Brainstem | Maximum dose | | is less than | 600.0 | 3000.0 | Remove |
| <input type="checkbox"/> | SFRT Anu | Cauda E... | Maximum dose | | is less than | 620.0 | 3100.0 | Remove |
| <input type="checkbox"/> | SFRT Anu | Sacral Pl... | Maximum dose | | is less than | 640.0 | 3200.0 | Remove |
| <input type="checkbox"/> | SFRT Anu | Great Ve... | Maximum dose | | is less than | 1000.0 | 5000.0 | Remove |
| <input type="checkbox"/> | SFRT Anu | Trachea | Maximum dose | | is less than | 800.0 | 4000.0 | Remove |
| <input type="checkbox"/> | SFRT Anu | Bronchi | Maximum dose | | is less than | 600.0 | 3000.0 | Remove |
| <input type="checkbox"/> | SFRT Anu | Ribs | Maximum dose | | is less than | 1100.0 | 5500.0 | Remove |
| <input type="checkbox"/> | SFRT Anu | Skin | Maximum dose | | is less than | 600.0 | 3000.0 | Remove |
| <input type="checkbox"/> | SFRT Anu | Bile Duct | Maximum dose | | is less than | 800.0 | 4000.0 | Remove |
| <input type="checkbox"/> | SFRT Anu | Duoden... | Maximum dose | | is less than | 500.0 | 2500.0 | Remove |
| <input type="checkbox"/> | SFRT Anu | Ureter | Maximum dose | | is less than | 900.0 | 4500.0 | Remove |

Figure 13: Maximum point doses for serial organs.

| | | |
|---|-----------|--|
| R | Femurs | $D_{10.0 \text{ cm}^3} < 3000 \text{ cGy}$ |
| R | Kidneys | $D_{200.0 \text{ cm}^3} < 2800 \text{ cGy}$ |
| R | Liver | $D_{700.0 \text{ cm}^3} < 2000 \text{ cGy}$ |
| R | Lungs-GTV | $D_{30.0 \%} < 1300 \text{ cGy}$ |
| R | Lungs-GTV | $D_{1500.0 \text{ cm}^3} < 1200 \text{ cGy}$ |
| R | Lungs-GTV | $D_{1000.0 \text{ cm}^3} < 1300 \text{ cGy}$ |

Figure 14: Volumetric objectives for parallel organs.

2.2.5) Quality Assurance

The integrity and deliverability of the plans created on the prior patient scans were evaluated per SBRT QA protocol used in the clinic. The 2-dimensional External Portal Imaging Device (EPID) was used to measure fluence maps for each arc and compared against the calculated fluence maps using 95% pass rate for 3%/2mm gamma analysis criteria.

3) RESULTS

3.1) GRID Therapy

3.1.1) Physical GRID Block

3.1.1.1) Dosimetric Characteristics of the Block

Figure 15 shows the diameter of the hole and center to center spacing measured in Eclipse. The grid hole diameter was measured at 50% of the maximum dose and measured to be 1.49cm in the horizontal direction and 1.51 cm in the vertical direction (Figure 16) using RIT, which is in good agreement with hole diameter 1.43 cm at the isocenter measured in Eclipse TPS. The grid center to center spacing was measured to be 2.14 cm using a EBT3 film at isocenter using RIT (Figure 17), which is in good agreement with the grid spacing of 2.11 cm measured in Eclipse TPS. The transmission factor was set to be 15% in the block properties of TPS after setting up different values for it and comparing the film profiles with the dose plane from the isodose plan created in the Eclipse TPS.

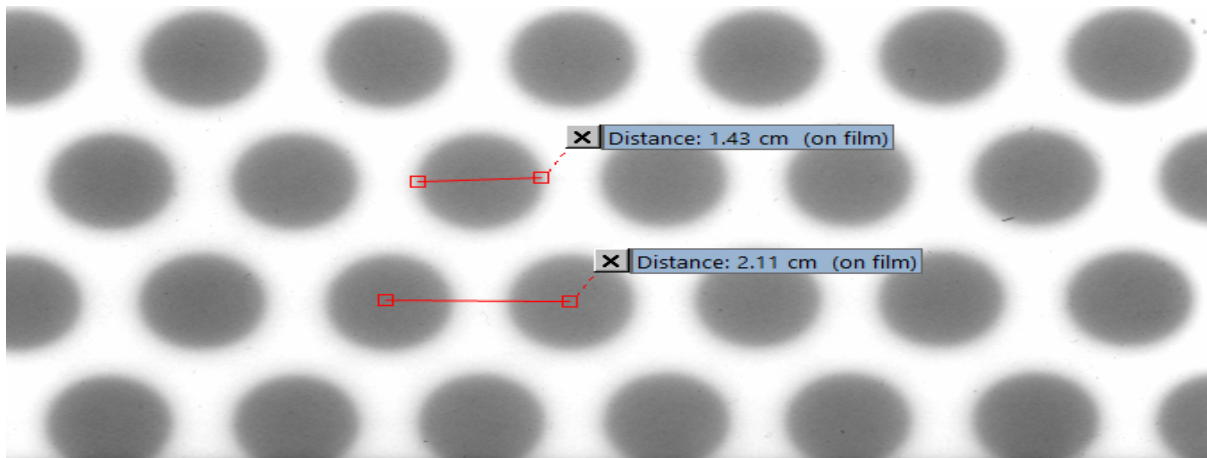


Figure 15: Diameter of the hole and center to center spacing. Hole diameter is 1.43 cm and grid spacing is 2.11cm (measured in Eclipse TPS).

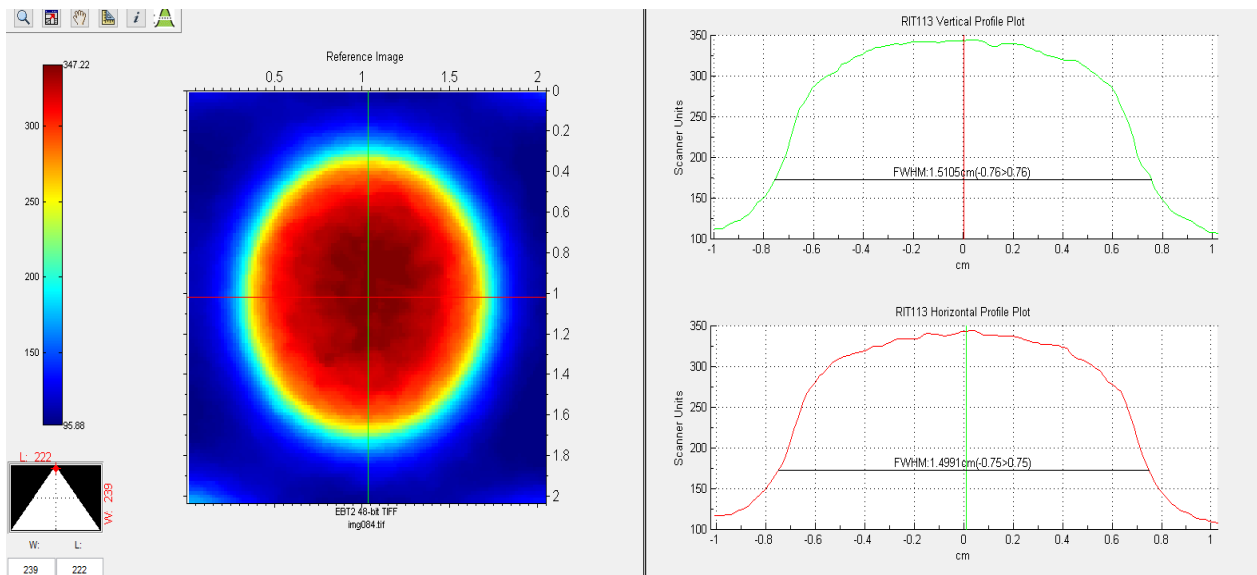


Figure 16: Hole diameter measured using RIT. It is 1.49 cm in horizontal direction and 1.51 cm in vertical direction (measured at 50% of maximum dose). Hole diameter at the isocenter mentioned in the Dot Decimal manual is 1.43cm. Our results are in good agreement with the specified diameter.

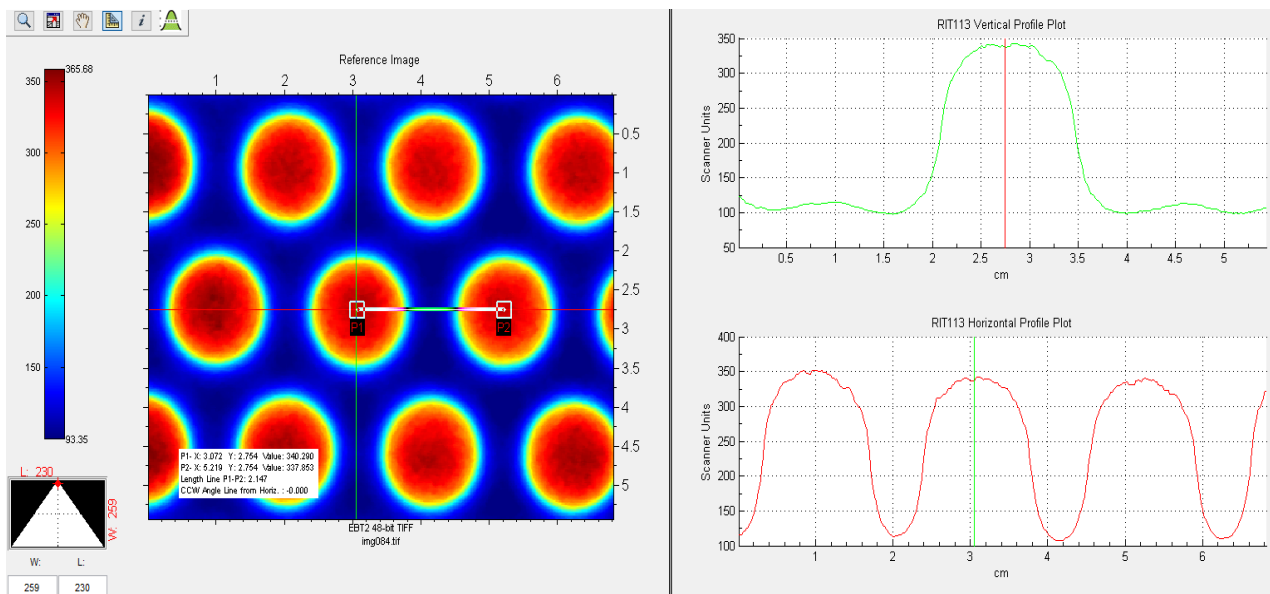


Figure 17: Center to center spacing measured using RIT. It is 2.14 cm at isocenter, and the Dot Decimal manual specifies it as 2.11 cm, which shows good agreement.

Figures 18-19 shows excellent agreement of the inline and cross line beam profiles for depths d_{max} and 5cm when comparing film to Eclipse TPS. Table 1 shows that point dose measured at different depths for the central hole are within 3% agreement with each other. The agreement between measured and calculated point dose values indicate that the beam quality calculated by Eclipse TPS matches with the beam quality produced by the grid block mounted on the linac. The dose to open region (hole) decreases with depth and dose to the blocked area is nearly constant with depth resulting in a decrease of PVDR as shown in Table 1.

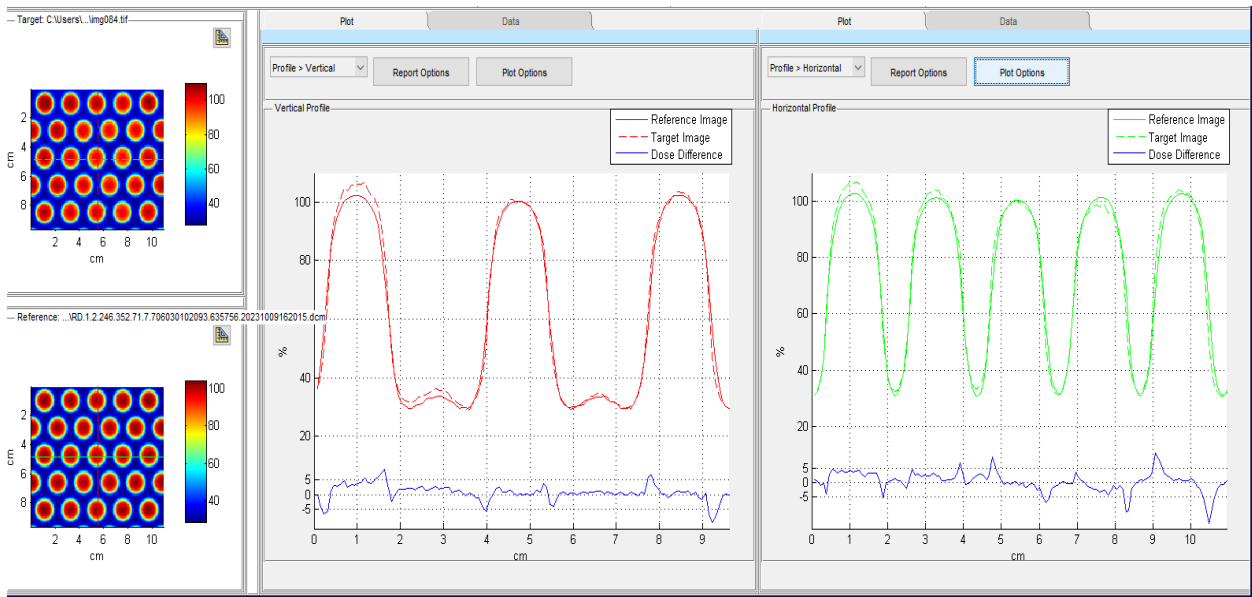


Figure 18: Vertical and horizontal beam profiles at d_{max} . This figure shows good agreement between the film (target Image) and planned dose (reference Image) from the TPS

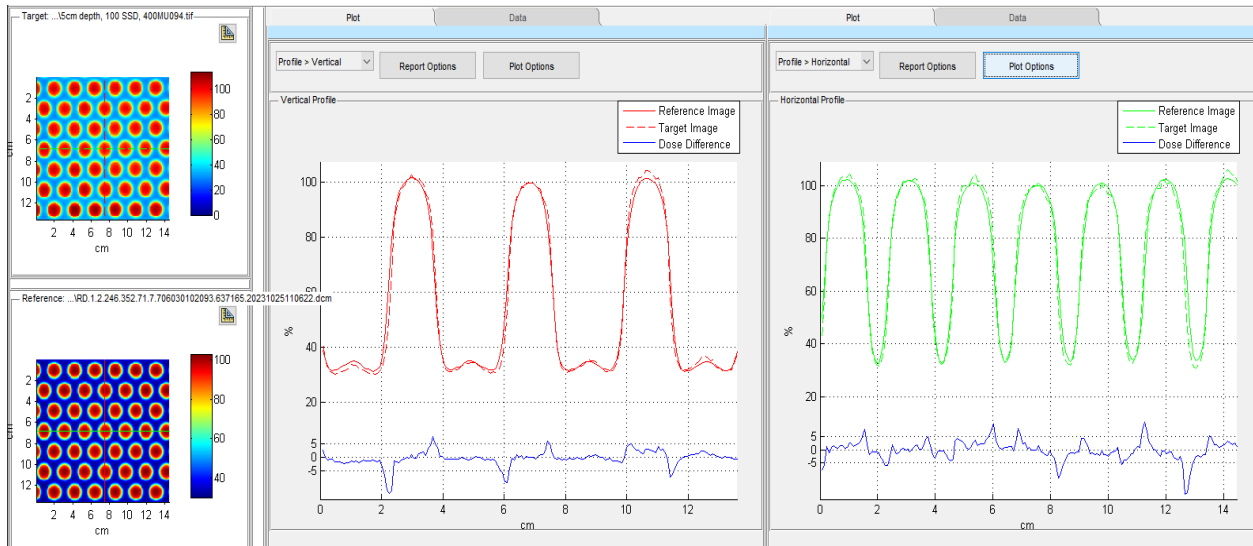


Figure 19: Vertical and horizontal beam profiles at depth 5cm. This figure shows good agreement between the film (target Image) and planned dose (reference Image) from the TPS.

| Depth (cm) | Film (cGy) Open area | TPS (cGy) Open area | Percent difference | Film (cGy) Blocked area | PVDR |
|---------------|-------------------------|------------------------|-----------------------|----------------------------|------|
| 2.3 cm (dmax) | 343.81 | 342.80 | 0.29 | 105.77 | 3.25 |
| 5 cm | 301.76 | 304.63 | 0.94 | 97.13 | 3.10 |
| 10 cm | 237.31 | 241.08 | 1.56 | 88.11 | 2.69 |
| 15 cm | 183.90 | 189.26 | 2.83 | 68.41 | 2.68 |

Table 1: Comparison between point doses measured using films and TPS at different depths.

The comparison of transverse beam and radial beam profiles for an 18x18 cm² open field versus grid field for a 10 MV beam are presented in Figures 20 and 21, respectively. The results show 100% output factor for an open field and 88% for a 10 MV beam at dmax which is in good agreement with the output factors shown in Table 2.

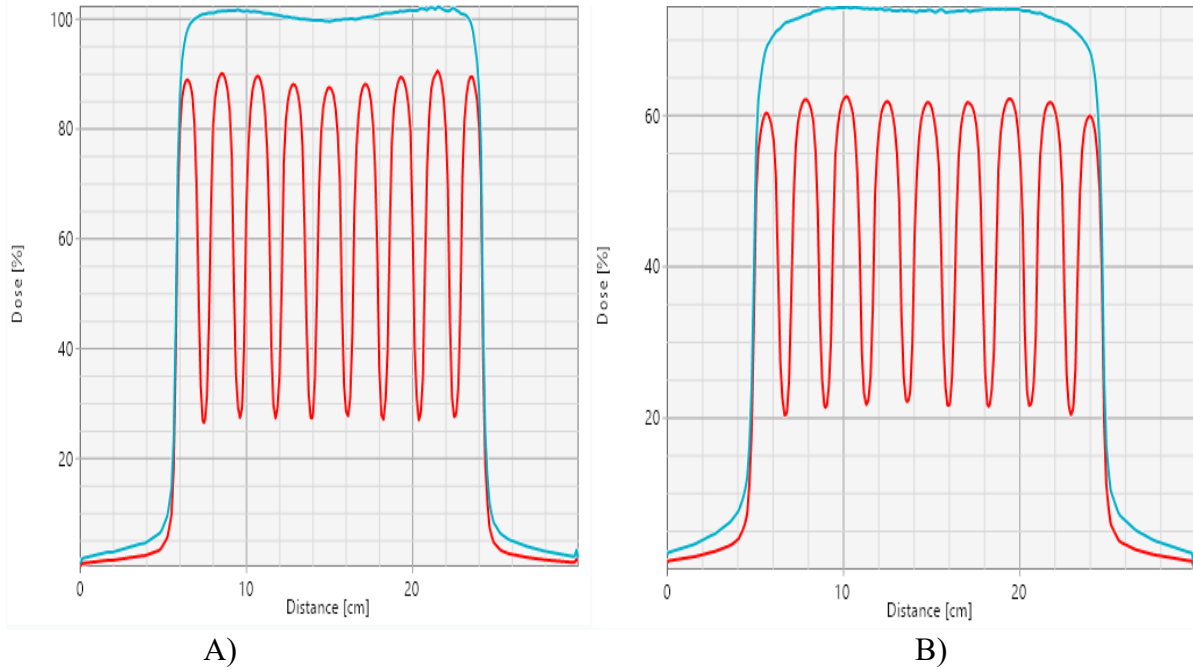


Figure 20: Comparison of transverse beam profiles for 10 MV beam at d_{max} (A) and 10 cm (B). Blue color represents an open field and red color represents grid field.

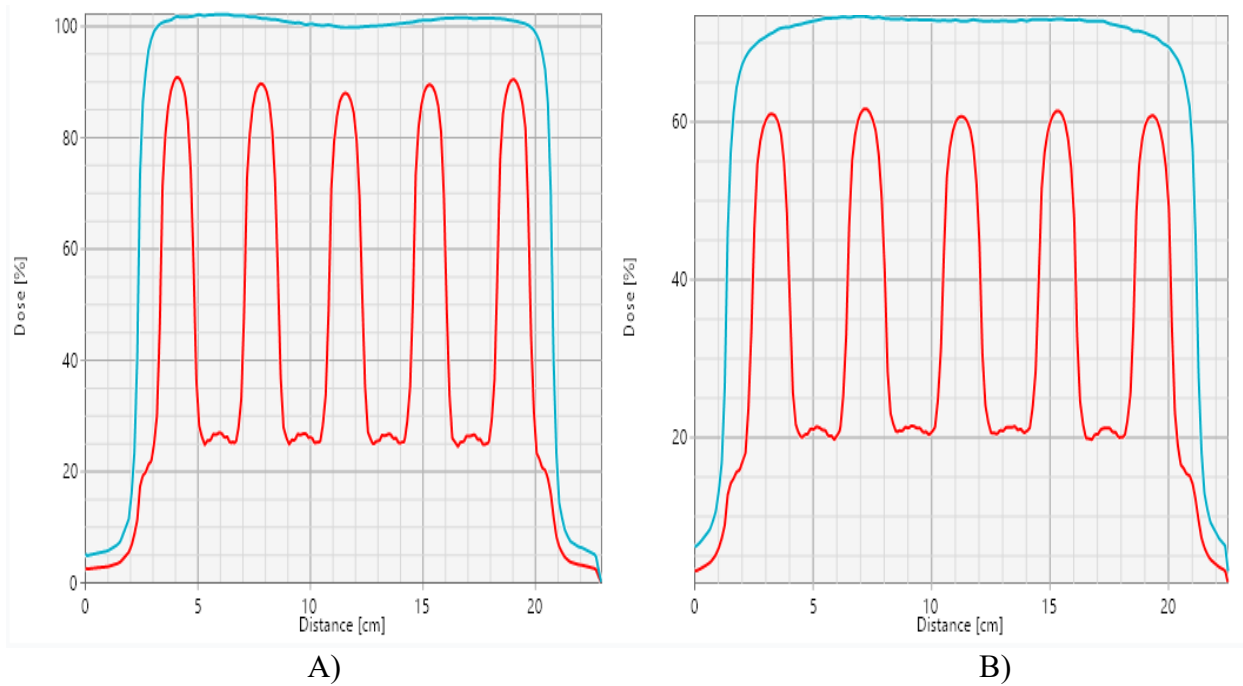


Figure 21: Comparison of radial beam profiles for 10 MV beam at d_{max} (A) and 10 cm (B). Blue color represents an open field and red color represents grid field.

Output factors were measured with a PTW microdiamond detector for 10 MV beam in water using grid block. These output factors are shown in Table 3. Comparison between this data was found to be consistent with the open field output factors summarized in Table 2.

| Field size | Grid output factor | Open field output factor |
|------------|--------------------|--------------------------|
| 4x4 | 0.828 | 0.911 |
| 6x6 | 0.839 | 0.950 |
| 10x10 | 0.857 | 1 |
| 15x15 | 0.879 | 1.031 |
| 18x18 | 0.890 | 1.045 |
| 20 x 20 | 0.898 | 1.053 |
| 25x25 | 0.914 | 1.069 |

Table 2: Comparison between grid output factors and open field output factors.

| | | | | | | | | | | |
|----|-------|-------|-------|-------|-------|-------|-------|-------|-------|-------|
| | 3 | 4 | 6 | 8 | 10 | 12 | 15 | 18 | 20 | 25 |
| 3 | 0.820 | 0.824 | 0.827 | 0.830 | 0.832 | 0.834 | 0.835 | 0.835 | 0.836 | 0.838 |
| 4 | 0.824 | 0.828 | 0.832 | 0.835 | 0.839 | 0.840 | 0.843 | 0.845 | 0.846 | 0.848 |
| 6 | 0.829 | 0.835 | 0.839 | 0.843 | 0.847 | 0.850 | 0.853 | 0.854 | 0.855 | 0.858 |
| 8 | 0.829 | 0.835 | 0.842 | 0.847 | 0.851 | 0.855 | 0.859 | 0.862 | 0.863 | 0.867 |
| 10 | 0.831 | 0.839 | 0.846 | 0.851 | 0.857 | 0.862 | 0.865 | 0.869 | 0.871 | 0.875 |
| 12 | 0.832 | 0.839 | 0.849 | 0.856 | 0.863 | 0.866 | 0.872 | 0.876 | 0.878 | 0.883 |
| 15 | 0.835 | 0.842 | 0.854 | 0.862 | 0.868 | 0.875 | 0.879 | 0.884 | 0.888 | 0.893 |
| 18 | 0.835 | 0.845 | 0.856 | 0.866 | 0.874 | 0.879 | 0.886 | 0.890 | 0.895 | 0.901 |
| 20 | 0.837 | 0.845 | 0.858 | 0.867 | 0.875 | 0.881 | 0.888 | 0.894 | 0.898 | 0.903 |
| 25 | 0.839 | 0.848 | 0.861 | 0.871 | 0.879 | 0.887 | 0.894 | 0.901 | 0.906 | 0.914 |

Table 3: Grid output factors. PTW microdiamond detector was used to measure output factors for 10 MV beam in water at depth of maximum dose for field sizes 3x3 cm² to 25x25 cm².

The blocked to open ratio for different field sizes, 10MV beam were measured using Gafchromic EBT3 film dosimetry and shown in Table 4.

| Field size(cm ²) | Blocked area (cGy) | Open area (cGy) | Blocked to open area (%) |
|------------------------------|--------------------|-----------------|--------------------------|
| 5x5 | 44.80 | 264.00 | 16.96 |
| 10x10 | 55.66 | 267.30 | 20.82 |
| 15x15 | 63.84 | 268.06 | 23.81 |
| 20x20 | 67.75 | 270.33 | 25.06 |
| 25x25 | 67.95 | 262.21 | 25.91 |

Table 4: Blocked to open area ratio for different field sizes.

The results for beam profiles, percentage depth dose, and output factors show that the evaluation of the dosimetric characteristics for the grid block in the Eclipse produce acceptable dosimetric accuracy.

3.1.1.2) Treatment Planning, Plan Evaluation Metrics

Figure 22 shows an example of dose profiles and dose distributions for three dimensional views of isodose color wash for a patient with osteosarcoma of right upper extremity. The target coverage constraints do not apply to grid therapy because of the non-uniform dose distribution. A physics working group recommended reporting several dosimetric quantities for the target (Zhang et al., 2020). These metrics are presented in Table 5. The primary treatment planning metrics to consider are PVDR (3 - 7), EUD (20 to 50% of the prescription dose) and maximum skin dose (30 Gy or <150% of the prescription dose) (Li et al., 2023). For the OAR constraints, the maximum

dose to each structure was limited to 6 Gy since there would be dose contribution from the following conventional radiation treatment. (Grams et al., 2023).

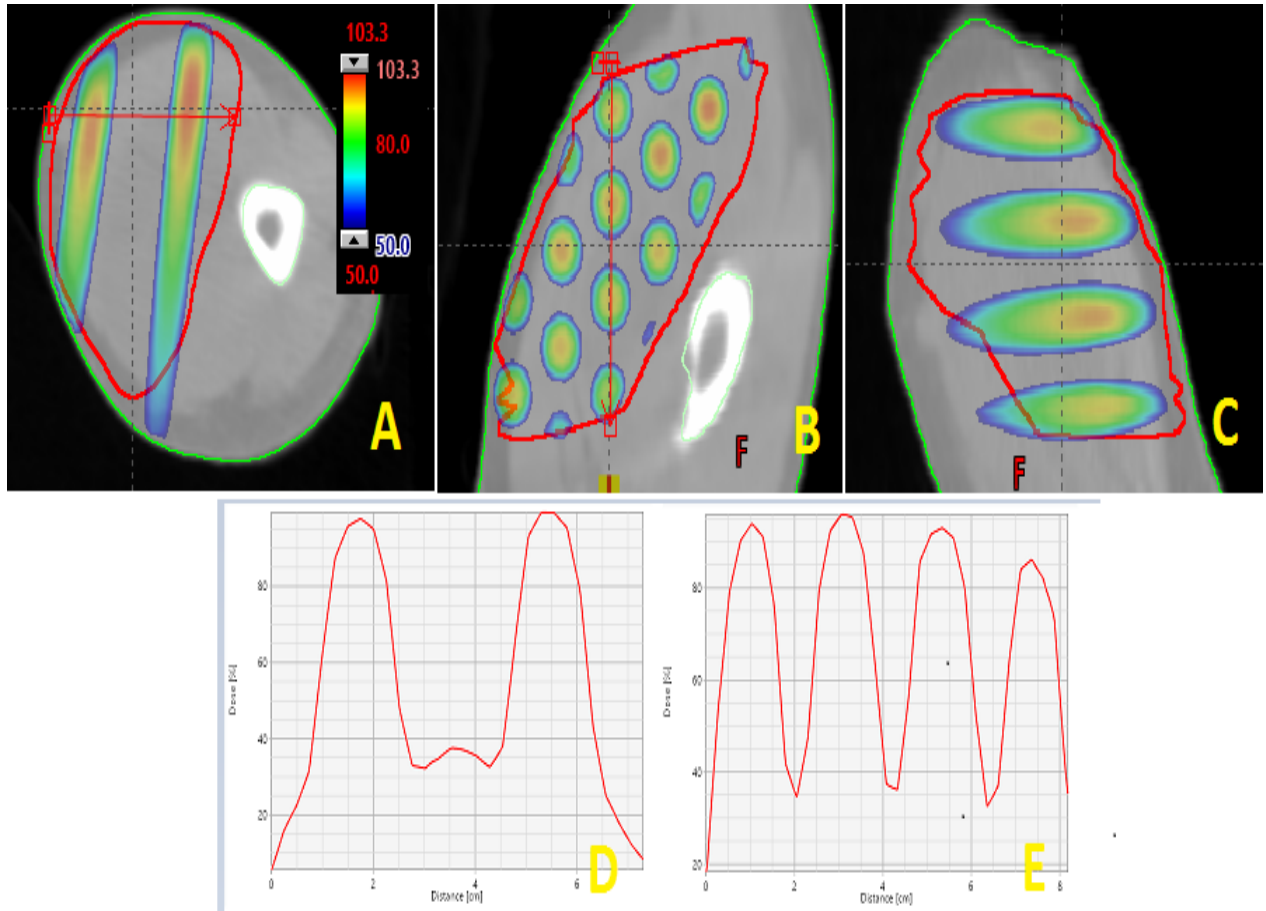


Figure 22: Views of isodose distribution for a physical block grid plan. Axial (A), coronal (B), sagittal (C) planes of a plan created for a patient with osteosarcoma of right upper extremity (GTV 371.04cc). Radial (D) and transverse (E) dose profiles taken through the center of high dose (peaks) and low dose (valleys).

| | Dosimetric parameters | 1 | 2 | 3 | 4 | 5 |
|----|---|-------|-------|-------|-------|----------|
| | Treatment site | Leg | Arm | Leg | Arm | Shoulder |
| 1 | Prescription dose (Gy) | 15 | 15 | 15 | 15 | 15 |
| 2 | EUD for tumor (Gy) (20% to 50% of Rx dose) (Li et al., 2023) | 3.80 | 3.80 | 3.80 | 3.80 | 3.80 |
| 3 | Output factor at prescription depth (Gy/MU) | 0.839 | 0.853 | 0.863 | 0.829 | 0.826 |
| 4 | Dose covering target (Gy). 90% | 2.32 | 4.1 | 2.17 | 2.54 | 3.31 |
| | 50% | 6.20 | 6.46 | 6.83 | 6.00 | 6.13 |
| | 20% | 10.72 | 10.75 | 11.77 | 10.97 | 10.60 |
| | 10% | 12.38 | 12.26 | 13.58 | 13.05 | 12.33 |
| | 5% | 13.26 | 13.25 | 14.30 | 13.96 | 13.52 |
| 5 | Mean dose of target (Gy) | 7.03 | 7.37 | 7.64 | 7.04 | 6.66 |
| 6 | PVDR ($D_{10\%}/D_{90\%}$) (3-7) (Li et al., 2023) | 5.33 | 3.00 | 6.25 | 5.13 | 5.87 |
| 7 | Peak dose (Gy) | 15.40 | 15.48 | 15.82 | 15.53 | 16.39 |
| | Valley dose (Gy) | 5.0 | 4.25 | 6.27 | 5.61 | 5.53 |
| 8 | Peak width (defined at 50% of the max peak dose) (cm) | 1.6 | 1.6 | 1.6 | 1.53 | 1.59 |
| 9 | Peak to peak distance (cm) | 2.2 | 2.2 | 2.09 | 2.14 | 2.14 |
| 10 | Maximum skin dose (Gy) (30 Gy or < 150% of Rx) (Li et al., 2023) | 14.89 | 13.05 | 13.99 | 12.47 | 14.34 |
| 11 | Dose to OAR (Gy) - Bone | 2.05 | 0.70 | 1.01 | 2.07 | 0.49 |
| 12 | MU | 1954 | 1906 | 2005 | 1974 | 1953 |

Table 5: Dosimetric parameters for physical block grid plans. (Zhang et al., 2020)

3.1.1.3) Quality Assurance

QA of the grid plans was performed by creating verifications plans in the solid water and comparing those MU to hand calculated MU. The point dose at dmax was obtained from the verification plans. Table 6 shows good agreement for dose verification between Eclipse TPS calculated MU and hand calculated MU.

| Field Name | Test | Test | Test | Test | Test |
|-----------------------|------------|-------------|------------|--------|-----------|
| Treatment site | Right leg | Arm | Left leg | Arm | shoulder |
| Beam energy | 10x | 10x | 10x | 10x | 10x |
| Point dose (cGy) | 1413 | 1541.8 | 1551.2 | 1542 | 1487 |
| Effective field size | 3.7 x 15.8 | 13.9 x 21.0 | 9.6 x 10.9 | 5 x 11 | 4.8 x 5.1 |
| Output factor | 0.842 | 0.888 | 0.857 | 0.839 | 0.832 |
| Dmax (cm) | 2.3 | 2.3 | 2.3 | 2.3 | 2.3 |
| SSD (cm) | 100 | 100 | 100 | 100 | 100 |
| Inverse square factor | 0.955 | 0.955 | 0.955 | 0.955 | 0.955 |
| Expected TPS MU | 1730 | 1857 | 1917 | 1901 | 1846 |
| Calculated MU | 1756 | 1817 | 1894 | 1923 | 1870 |
| Percentage difference | 1.52 | -2.15 | -1.19 | 1.18 | 1.32 |

Table 6: QA for grid plans. Percentage difference between the MU calculated by the Eclipse TPS and the MU from hand calculation shows good agreement.

3.1.2) Virtual GRID using Multi leaf collimator

3.1.2.1) Treatment Planning and Plan Evaluation Metrics

An example of dose distributions for a 3D MLC based SFRT plans for a GTV created in a cylindrical phantom and for a right buttock leiomyosarcoma are shown in Figure 23 and Figure 24, respectively. Table 7 shows the dosimetric parameters for 5 test plans. Table 8 shows the maximum dose to the critical structures (dmax) for those associated test plans.

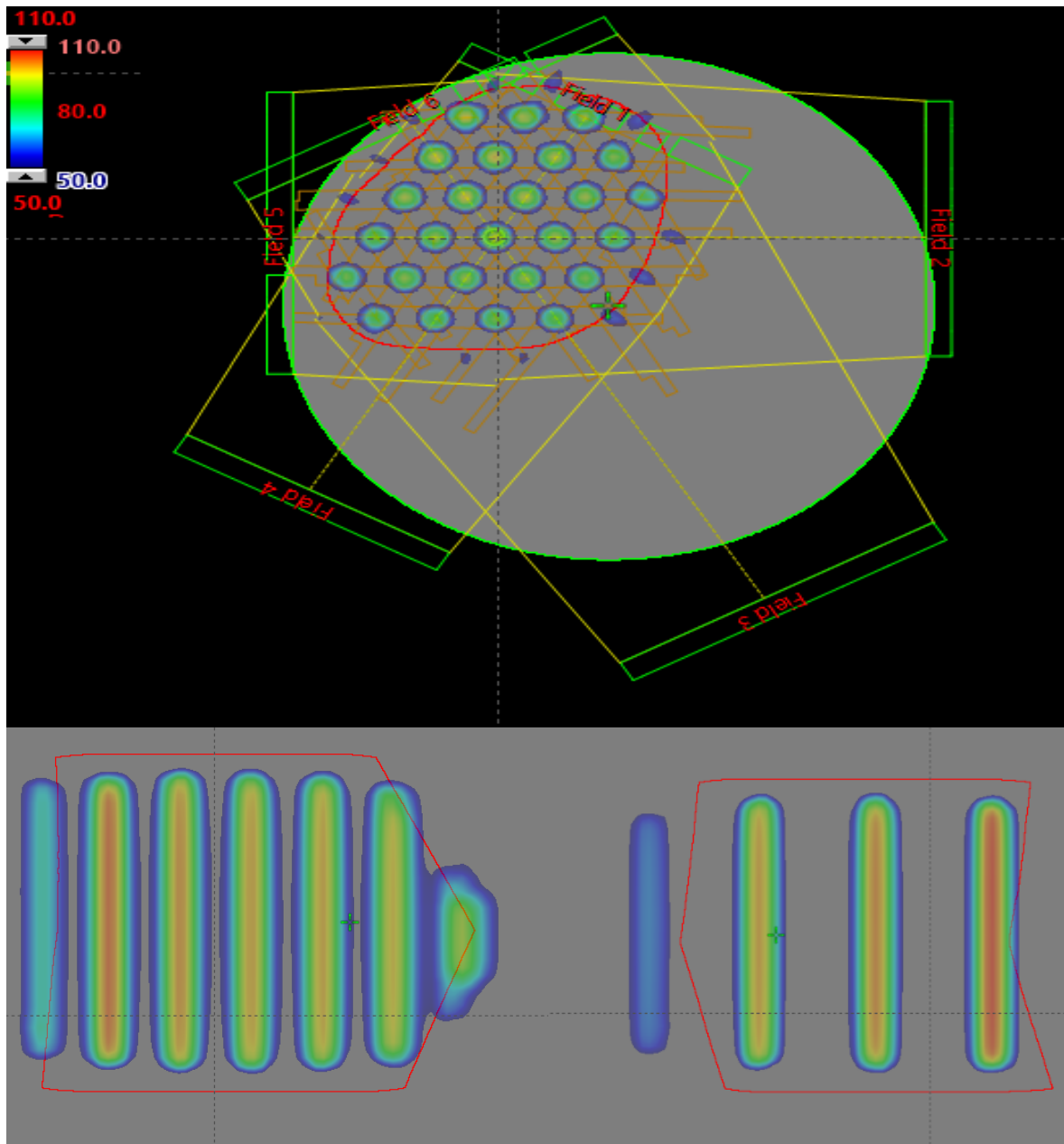


Figure 23: Views of isodose distribution for a 3D MLC based SFRT plan. Plan was created for a GTV (1549cc) in a cylindrical phantom with a single dose of 15Gy. All 6 gantry angles equally spaced were used to create the plan.

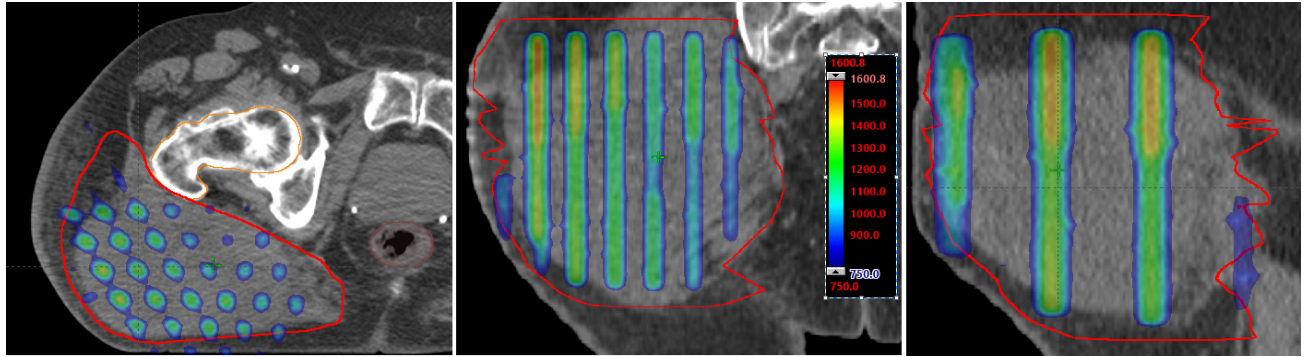


Figure 24: Views of isodose distribution for a 3D MLC based SFRT plan. Plan was created for a patient with right buttock leiomyosarcoma using a single dose of 15Gy (GTV 2598 cc, length 17cm) and hot spot of 106.7%. The OARs such as femur, rectum and bowel were spared. 5 out of 6 gantry angles were used to create the plan and 90 degree angle was not used due to large patient separation.

| Serial No. | Parameters | | 1 | 2 | 3 | 4 | 5 |
|------------|--|---------------|---------------|--------------|-------------|----------------|--------------|
| 1 | Treatment site | Phantom | Glute | Abd | Lung | Groin | Abd |
| 2 | GTV length, volume | 12.34, 1549cc | 17cm, 2598 cc | 12.80, 585cc | 11cm, 540cc | 10.49cm, 419cc | 9.74, 882 cc |
| 3 | MU, MU ratio | 2423, 1.61 | 2123, 1.41 | 2599, 1.73 | 2510, 1.25 | 2260, 1.50 | 2408, 1.60 |
| 4 | Dose Maximum (%) | 110 | 106.7 | 116 | 112.8 | 114 | 108.6 |
| 5 | PVDR $\left(\frac{GTVD10\%}{GTVD90\%}\right)$ (2.8-4.5) (Pokhrel et al.) | 2.97 | 2.85 | 2.89 | 2.94 | 2.87 | 2.81 |
| 6 | GTV(V7.5Gy) (50.5%-64.1%) (Pokhrel et al.) | 52.07 | 52.62 | 51.01 | 50.53 | 51.4 | 53.72 |
| 7 | Mean GTV Dose (7.3-9.1Gy) (Pokhrel et al.) | 8.03 | 7.93 Gy | 7.97 | 7.86 | 7.66 | 7.94 |

Table 7: Dosimetric parameters for 3D MLC based SFRT plans.

| Organ | Constraint (Gy) (AAPM TG-101) | 1 | 2 | 3 | 4 | 5 |
|-----------------|----------------------------------|-------|-------|-------|-------|-------|
| Skin | Dmax<27.5 | 13.33 | 9.94 | 7.76 | 11.50 | 8.12 |
| Bowel | Dmax<22 | 7.61 | 14.53 | - | 3.2 | 8.49 |
| Kidneys | V9.5<200cc | 0 | 0 | - | - | 0 |
| Spinal cord | Dmax<14 | - | 0.19 | 8.6 | - | 7.33 |
| Bladder | Dmax<25 | 7.71 | - | - | 3.7 | 0.028 |
| Esophagus | Dmax<15.4 | - | - | 7.04 | - | 0.08 |
| Fem heads | V15<10cc | 0 | 0 | - | 0 | 0 |
| Great Vessels | Dmax<37 | - | - | 13.97 | - | 2.66 |
| Heart | Dmax<22 | - | - | 4.16 | - | 0.03 |
| Brachial Plexus | Dmax<16.4 | - | - | 9.9 | - | - |
| Liver-GTV | V11<700cc | 0 | 0 | 0 | - | 0 |
| Lungs-GTV | V7.6<1000cc | - | - | 3.45 | - | 0 |
| | V7<1500cc | - | - | 0 | - | 0 |
| | V8<37% | - | - | 0 | - | 0 |
| Rectum | Dmax<30 | 3.34 | 0.06 | - | 0.96 | 0.028 |
| Ribs | Dmax<33 | - | - | 16.18 | - | - |
| Stomach | Dmax<22 | - | - | - | - | 0.12 |
| Trachea | Dmax<13.3 | - | - | 7.74 | - | 0 |

Table 8: Doses to the critical structures for 3D MLC based SFRT plans.

3.1.2.2) Quality Assurance

An example of the MU per treatment field verification using third party software Clear Check (Radformation, Inc., New York, NY) is shown in Figure 25. The difference between MU calculated by Eclipse TPS and the Clear Check software was within 5%.

MU Results

| Field ID | Calculation Point | TPS MU | ClearCalc MU | Difference | Pass/Fail | Verify | Comment |
|----------|-------------------|---------|--------------|------------|-----------|--------|---------|
| Field 1 | Isocenter 1 | 390.1MU | 394.3MU | 1.08% | ✓ | | |
| Field 2 | Isocenter 1 | 455.1MU | 445.2MU | -2.18% | ✓ | | |
| Field 3 | Isocenter 1 | 464.7MU | 457.8MU | -1.48% | ✓ | | |
| Field 4 | Isocenter 1 | 393.6MU | 384.4MU | -2.34% | ✓ | | |
| Field 5 | Isocenter 1 | 356.4MU | 345.0MU | -3.20% | ✓ | | |
| Field 6 | ClearCalc Point 1 | 363.3MU | 360.0MU | -0.91% | ✓ | | |

Figure 25: Second MU check for a 3D MLC based SFRT plan.

3.2) Lattice Therapy

3.2.1) Treatment Planning and Plan Evaluation Metrics

The 3D dose distribution and dose profile for a LRT plan with an abdominal mass (GTV 565.4cc) are shown in Figures 26 and 27; while Figures 28 and 29 present the 3D dose distribution and profiles for a patient with liposarcoma of the right peritoneum (GTV 3445 cc). Figure 27 and Figure 29 show no dose bridging between the high dose spheres for axial, sagittal and coronal viewing planes above 80%. PTV_6670 and PTV_2000 achieved greater than 95% coverage while sparing the OAR for all the LRT test plans as shown in Table 9. If PTV_6670 high dose sphere caused an OAR to exceed clinical objectives, that sphere was removed or retracted up to 3mm. The maximum dose to the OARs is shown in Table 10.

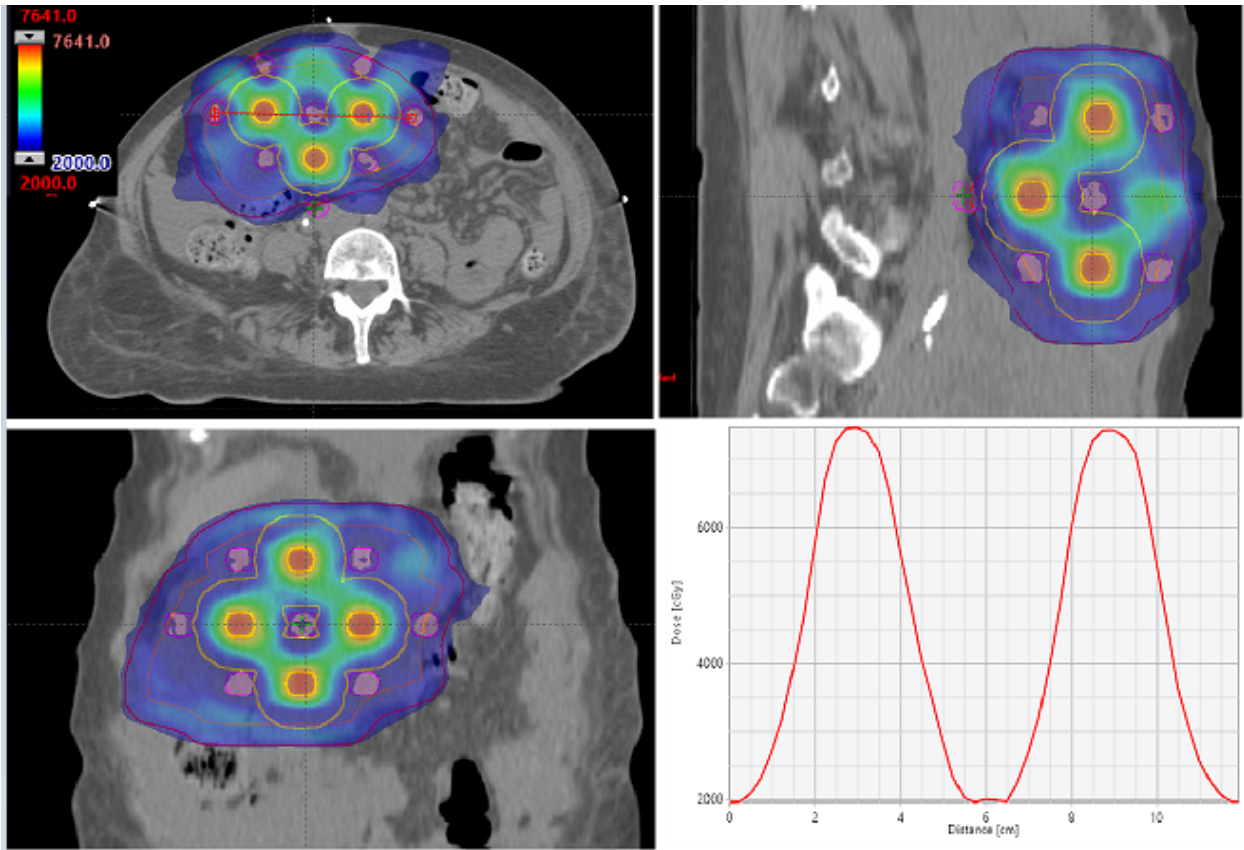


Figure 26: Views of isodose distribution for a LRT plan. Axial (A), sagittal (B), coronal (C) planes of a plan created for a patient with abdominal mass (GTV 565.4 cc). Dose profile (D) taken through the center of high and low dose spheres in axial plane. GTV_2000 (Orange), PTV_2000 (Red), DR_1.5 (Yellow) contours are also shown.

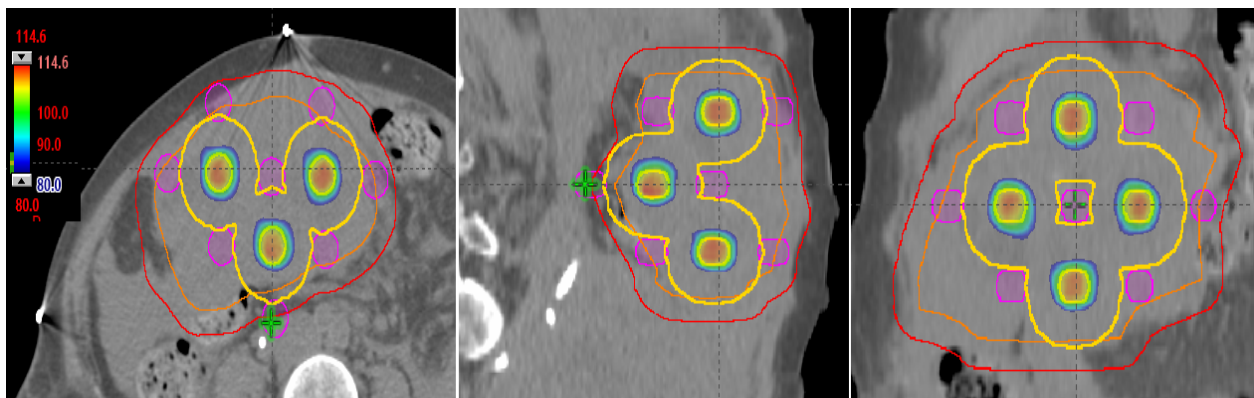


Figure 27: Views of isodose distribution showing no dose bridging between high dose spheres.

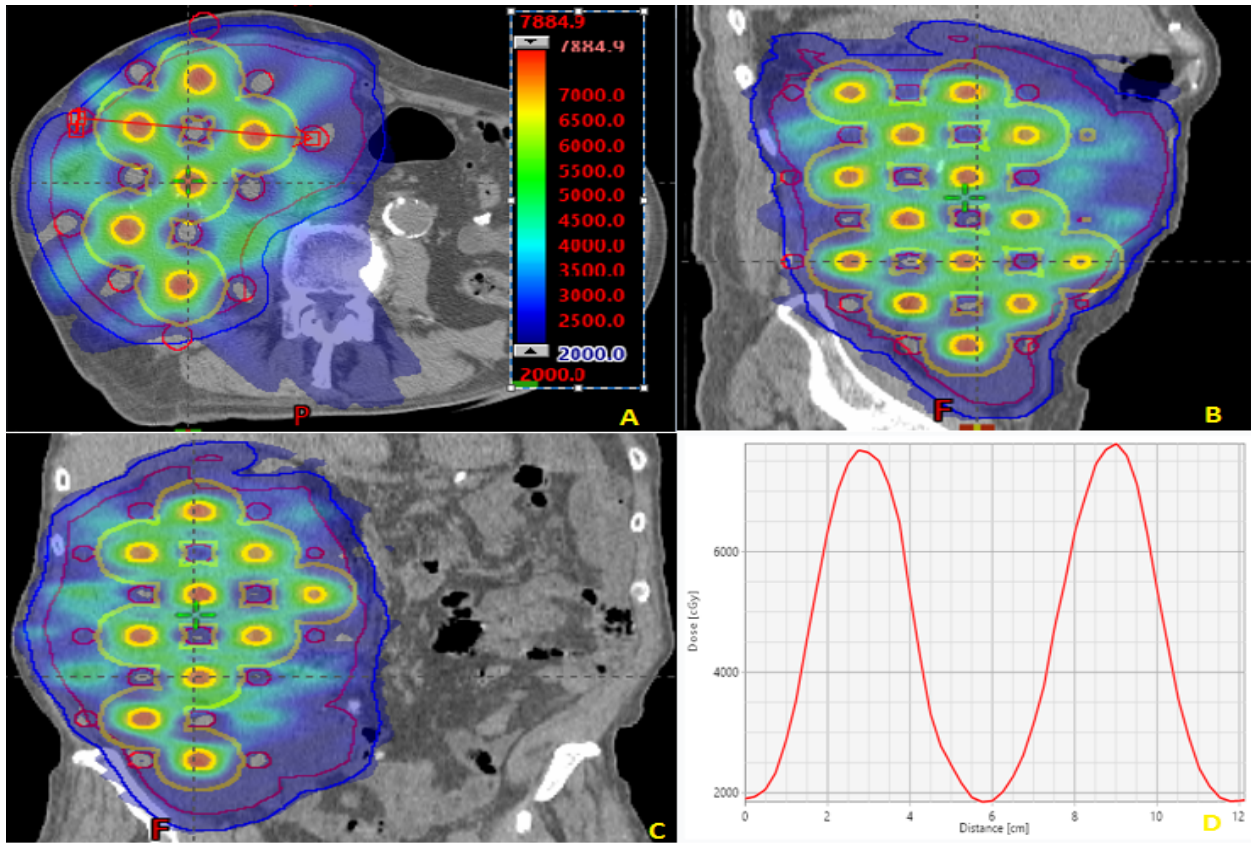


Figure 28: Views of isodose distribution for a LRT plan. Axial (A), sagittal (B), coronal (C) planes of a plan created for a patient with liposarcoma of the right retroperitoneum (GTV 3445 cc). Dose profile (D) taken through the center of high and low dose spheres in axial plane. GTV_2000 (Red), PTV_2000 (Blue), DR_1.5 (Yellow) contours are also shown.

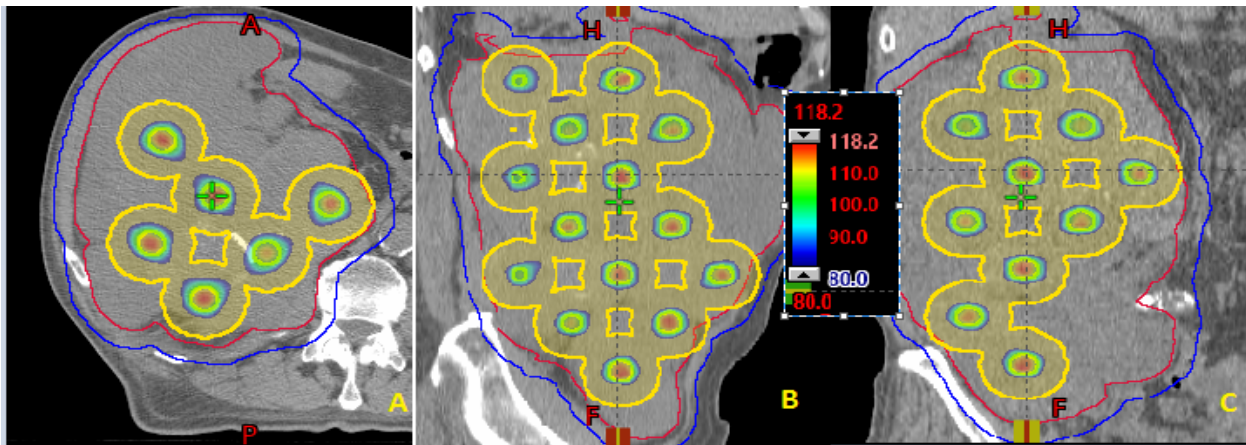


Figure 29: Views of isodose distribution showing no dose bridging between high dose spheres.

| Coverage Metrics | | Min-Max (Kavanaugh et al.) | 1 | 2 | 3 | 4 | 5 |
|--|----------------------------------|--------------------------------------|---------|---------|---------|--------|---------|
| site | | | Abd | Abd | Abd | Lung | glut |
| GTV cc | | | 585.4 | 3445 | 2481.5 | 540.8 | 2598 |
| GTV length | | | 12.80 | 15.56 | 12.34 | 9.10 | 20.77 |
| $\frac{PTV_{6670}}{GTV_{2000}}$ | | | 1.5 | 1.5 | 1.9 | 1.4 | 1.2 |
| MU Ratio | | 2 – 4 (Up to 6 for GTV>2000cc) | 2.83 | 4.93 | 5.90 | 3.03 | 4.23 |
| Hot spot (%) | | <120 | 114.5 | 118.2 | 117.5 | 113.1 | 116.5 |
| PTV_6670 | Max (Gy) | 72.9-79.6 | 75.42 | 78.84 | 78.35 | 75.42 | 77.71 |
| | Mean (Gy) | 68.9-72.8 | 72.31 | 71.20 | 71.65 | 72.31 | 71.39 |
| | V _{100%Rx} (%) | 95.2-100 | 100 | 95.66 | 98.86 | 100 | 98.17 |
| | V _{95%Rx} (%) | 97.2-100 | 100 | 100 | 100 | 100 | 100 |
| | #Spheres | 1-34 | 5 | 34 | 32 | 5 | 21 |
| PTV_2000 | PTV_2000cc | - | 892.42 | 5033.16 | 4572.71 | 892.42 | 4472.02 |
| | V _{100%rx} cc (body) | - | 1259.56 | 6498.51 | 5899.19 | 1263.2 | 5916.22 |
| | C.I | 0.9-1.8 | 1.41 | 1.29 | 1.29 | 1.41 | 1.32 |
| | V _{100%Rx} (%) | 82.1-100 | 99.37 | 98.98 | 96.76 | 99.37 | 99.30 |
| | V _{95%Rx} (%) | 94.8-100 | 100 | 100 | 100 | 100 | 99.95 |
| PTV_Avoid | Mean | 19.4-23.2 | 20.20 | 22.39 | 20.88 | 20.20 | 21.84 |
| | V _{18Gy} (%) | 95.1-100 | 100 | 100 | 99.5 | 100 | 100 |
| | Max (Gy) | 21.1-39.7 | 23.25 | 39.0 | 33.52 | 23.25 | 34.00 |
| Gradient Metrics (1.5cm Ring) | Mean (Gy) | 28.6-45 | 38.39 | 42.01 | 40.28 | 38.39 | 41.97 |
| | Median (Gy) | 25.2-44.9 | 36.84 | 41.55 | 39.71 | 36.84 | 41.44 |
| | St Dev (Gy) | 9.7-12.5 | 9.32 | 9.57 | 9.95 | 11.06 | 10.20 |
| | DR 1.5 | 2.4-4.6 | 3.95 | 4.34 | 3.99 | 3.33 | 4.06 |
| GTV-1cm | Dp/Dmean | 3-3.5 | 3.18 | 3.0 | 3.25 | 3.24 | 3.15 |
| GTV_2000 | EUD(Gy) | 22.3-26.3 | 25.27 | 26.01 | 25.41 | 24.70 | 25.08 |
| | DR | 3-3.7 | 3.57 | 3.17 | 3.43 | 3.57 | 3.26 |
| | V _{50Gy} (cc) | 6.1-426.4 | 40.51 | 342.68 | 272.4 | 40.51 | 239.35 |
| | V _{50Gy} (%) | 5.9-19.0 | 7.49 | 9.98 | 10.97 | 7.49 | 9.18 |
| | D _{90%} (Gy) | 20.1-24 | 22.28 | 23.15 | 22.79 | 22.29 | 22.27 |
| | D _{50%} (Gy) | 23.8-35.3 | 27.59 | 33.73 | 34.14 | 27.61 | 31.16 |
| | D _{10%} (Gy) | 41.8-64.4 | 46.46 | 49.97 | 50.91 | 46.43 | 49.17 |

Table 9: Dosimetric parameters for LRT plans.

| Organ | Constraint (Gy) (AAPM TG-101) | 1 | 2 | 3 | 4 | 5 |
|-----------------|----------------------------------|-------|----------|-------|--------|-------|
| Skin | Dmax<38.5 | 28.58 | 36.26 | 33.81 | 19.07 | 37.39 |
| Bowel | Dmax<35 | 32.27 | 32.63 | 32.81 | - | 20.71 |
| Kidneys | V18<200cc | 0 | 136.71cc | 173cc | - | 0 |
| Spinal cord | Dmax<28 | 4.90 | 26.30 | 22.95 | 18.17 | - |
| Bladder | Dmax<38 | 11.47 | 2.96 | - | - | 20.71 |
| Duodenum | Dmax<26 | - | - | 22.45 | - | - |
| Esophagus | Dmax<35 | - | 7.93 | 23.58 | 26.65 | - |
| Fem heads | V30<10cc | 0 | 0 | - | - | 0 |
| Great Vessels | Dmax<53 | - | 27.26 | 36.10 | 31.52 | - |
| Heart | Dmax<38 | - | 1.16 | 22.90 | 28.89 | - |
| Brachial Plexus | Dmax<32 | - | - | - | 30.19 | - |
| Liver-GTV | V21<700cc | 4.57 | 64.47cc | 0 | 0 | 0 |
| Lungs-GTV | V13.5<1000cc | - | 0 | - | 281.75 | - |
| | V12.5<1500cc | - | 0 | - | 302 | - |
| | V13.5<37% | - | 0 | - | 32.51 | - |
| Rectum | Dmax<38 | 3.74 | 3.12 | - | - | 19.49 |
| Ribs | Dmax<57 | - | - | 41.15 | 47.09 | - |
| Stomach | Dmax<35 | - | 12.14 | 31.67 | - | - |
| Trachea | Dmax<33 | - | 0.26 | - | 30.87 | - |

Table 10: Doses to the critical structures for LRT plans.

3.2.2) Quality Assurance

The VMAT plans created using LRT technique passed QA testing with greater than 95% passing rate per a SBRT QA protocol with EPID portal dosimetry at 3%/2mm. Figure 30 shows excellent agreement between the measured and the calculated fluence maps for the patient diagnosed with a left retroperitoneal liposarcoma with GTV 2481.5 cc.

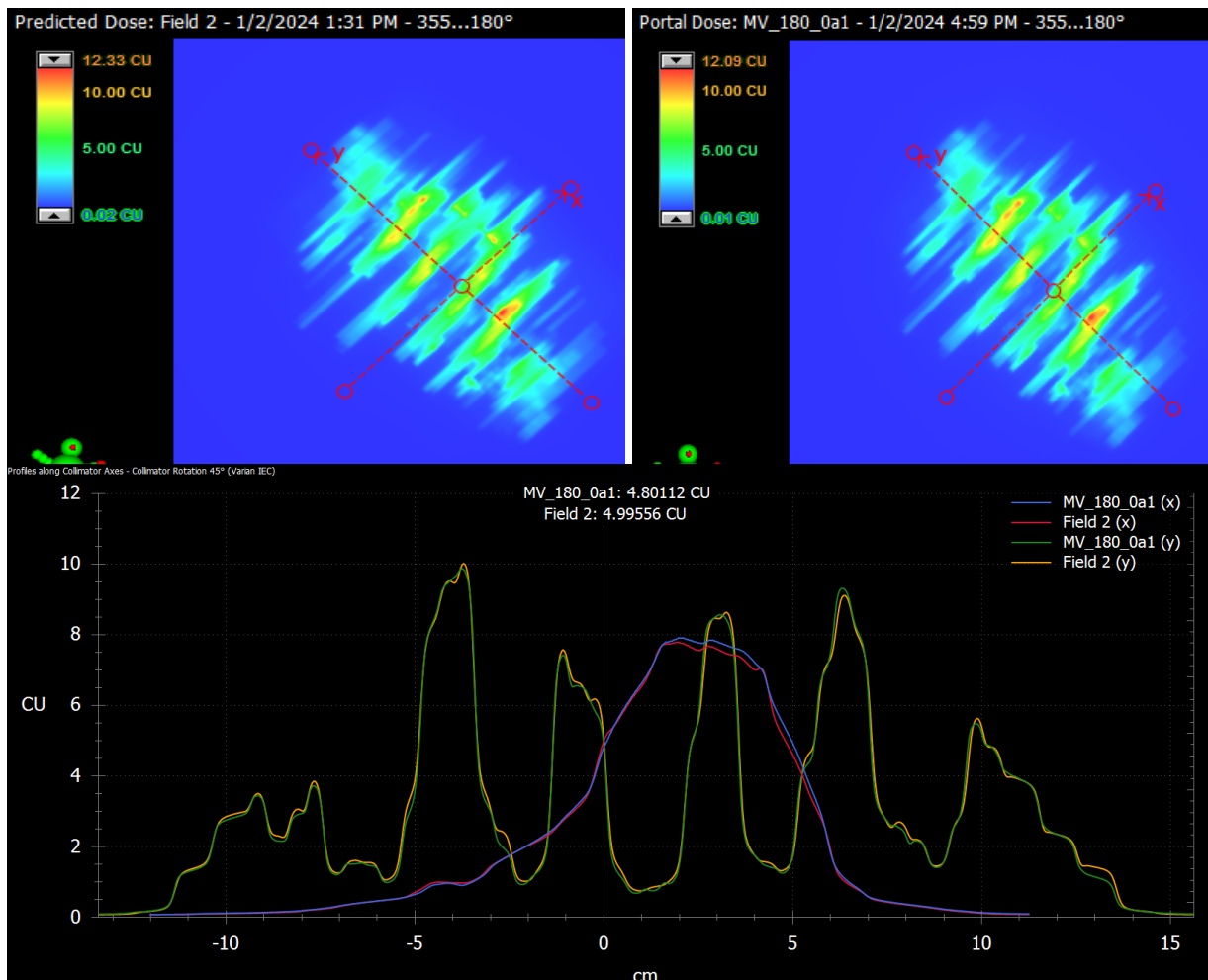


Figure 30: QA for a LRT plan showing predicted and portal dose. Comparison of the profiles along collimator axes shows 100% passing rate for 3%/2mm criteria.

4) DISCUSSION

SFRT was developed to treat bulky tumors that are challenging to be controlled with conventional fractionated radiation due to the difficulty of delivering high doses to the tumor while limiting the surrounding normal tissue toxicity. Local tumor control was achieved by creating open and closed radiation areas as it was known that small volumes of tissues can tolerate high doses (Mohiuddin et al., 1999). The advantage of using grid therapy is better repair capability of normal tissues (Zhang et al., 2007). SFRT using megavoltage beams mimics the dose distribution of high dose brachytherapy allowing the delivery of high doses like those used in SBRT (Mohiuddin et al., 1999). Kaiser et al. (2013) reported dramatic response from neoadjuvant SFRT for large, high grade extremity sarcoma with 90% tumor regression rate and 99% necrosis rate which decreases the need for chemotherapy.

To define the optimal arrangement of the hole diameter and spacing in the grid blocks, Gholami et al. (2016) performed Monte Carlo simulations to simulate 25 different grid block patterns. The results show that a hole diameter between 1cm and 1.25 cm could be used to achieve optimum clinical results based on improved TR for the grid block and that a hole separation distance of 1.7cm achieved maximum TR. Further, increasing the spacing between the grid holes kept TR nearly unchanged. Zwicker et al. (2004) showed no significant dependence of TR on grid spacing. The grid hole diameter and grid spacing for the physical grid block at ICC were measured to be 1.43cm and 2.11, respectively. Because TR analysis was outside the scope of this project, it is difficult to ascertain how the grid hole diameter and grid spacing of the ICC physical block would have affected this parameter.

Mohiuddin et al. (1999) showed doses $\geq 15\text{Gy}$ achieved a 94% palliative response versus 62% for doses $< 15\text{Gy}$. The response was higher when the treatment was followed by a uniform

2Gy per fraction ($> 40\text{Gy}$) to the target volume using 3D conformal or VMAT technique (92%), compared to grid therapy alone (86%). It has been speculated that the high dose grid fraction induced reoxygenation that improves outcome of the following conventional radiation therapy (Mohiuddin et al., 1999). Gholami et al. (2016) reported the TR value increases with prescribed dose in grid therapy and showed TR value to be 2.8, 2.03, and 1.45 for prescribed dose of 20 Gy, 15 Gy, and 10 Gy for a radioresistant tumor with survival fraction of 0.55. Zhang et al. (2008) showed that 15Gy single fraction grid therapy can increase normal cell survival ratio by at least 37% compared with open field debulking radiation to the average normal tissue. Regardless of tumor depth, the prescription point for all single grid fields is d_{max} , which can cause less than optimal dose delivery for the deep lesions. If the prescription depth is increased to gain better therapeutic advantage, the dose to the overlaying normal tissues would increase. Alternatively, to increase the dose at depth for deep seated tumors, the parallel opposed beam setup can be used, which can shift the prescription point to deeper depths and exhibit better therapeutic advantage (Meigooni et al., 2007). With this technique, the spatially fractionated modulation can be preserved and dose to the tumor be increased. For the test treatment plans presented in this project, 15Gy was used as the prescription dose at ICC.

The virtual grid using MLC approach of delivering SFRT is easy to use as MLC is already incorporated in the linac head. However, virtual grid using MLC based approach takes longer time to deliver when compared with physical grid approach as a greater number of segments are required to cover the target which increases the number of MU (Buckey et al.,2010). Also, the virtual grid with MLC exhibits leakage in the field that smears out the low dose regions and negates the spatial fractionation that we want to exploit. (Buckey et al.,2010).

Using a physical grid block provides better PVDR compared to a virtual grid. Grid therapy is the fastest way of delivering SFRT treatments and creating a plan in the Eclipse TPS can help visualize 3D dose distribution to the target and OAR. However, there are some limitations in using physical grid. Firstly, physical grid is heavy to use for the therapists which poses safety concerns and there is risk for the patients from the heavy block at certain angles. Secondly, deep seated tumors may not receive the prescribed dose and escalation of tumor dose is difficult to achieve while sparing critical organs and managing skin toxicity. Thirdly, it is not available in all clinics and needs to be commissioned in the TPS to get the dosimetric details to evaluate the plan.

The 3D MLC based SFRT technique enhances doses to the deep-seated tumors while sparing adjacent OAR. It eliminates the risk for the therapists from using heavy physical grid. This technique allows for the fast and safe treatment for large and bulky tumors. It also allows quick debulking of unresectable large tumors and can aid in pain relief.

For grid plans using the physical block, the expected range for PVDR is 3 - 7. As shown in Table 5, the PVDR for all the test plans is within this expected range. The maximum skin dose constraints for the grid plan is 30 Gy or $< 150\%$ of prescription dose and EUD for the tumor should be between 20% - 50% of the prescription dose. All test plans met both the constraint for maximum skin dose and tumor EUD. For all the virtual grid plans, PVDR (2.8 - 4.5), mean GTV dose (7.3 - 9.1 Gy), and GTV(V7.5Gy) (50.5 % – 64.1 %) are within the expected range as shown in Table 7.

LRT technique was used to treat cancers in chest and pelvis (Amendola et al., 2019; Amendola et al., 2020). There was statistically significant reduction in tumor size and long overall patient survival rate when they safely delivered LRT to patients with advanced stage non-small cell lung cancer. LRT can be used either for palliative tumor debulking or inducing anti-tumor

immunity in combination with immune checkpoint blockade treatment (Wu et al., 2020). A phase 1 trial of lattice SBRT for large tumors demonstrated improved global health at 14 days after treatment and improvement was preserved at 90 days. Even though the patients had very large tumors, the GTV significantly shrunk over a median time of 81 days after receiving LRT (Duriseti et al., 2022). Data also showed that patients did not experience any increased toxicity with this approach. However, the late toxicity associated with this approach was not evaluated. The change in cytokines reported in this study showed that the LRT induces immune-mediated response. This study supports further investigation in the clinical trials of LRT. It was noted that EUD has not been a widely established parameter to correlate the biological effects of SFRT as it only considers cell survival from radiation dose received by tumor cells and does not consider other effects causing cell death in the low dose regions (Li et al., 2023).

Amendola et al. (2019) reported a complete response in a patient with a large non-small cell lung cancer treated with LRT using a single fraction treatment plan which delivered 3 Gy to the PTV and 18 Gy to the three vertices (1.5 cm in diameter with center-to-center separation of 2cm created in 218.5 cc GTV including large LUL mass equivalent to 7.5 cm spherical diameter), followed by 29 fractions of 2 Gy per fraction (conventional fractionation) with concomitant chemotherapy. Further, Amendola et al. (2020) confirmed high tumor response and local tumor control of 100% (a median follows up of 16 months) in treating far advanced bulky cervical cancer patients using LRT plan that delivered 9Gy in 3 fractions to the PTV and 24 Gy in 3 fractions to the 5 vertices within GTV, followed by conventional fractionation (44.28 Gy in 1.8 Gy fractions). The 24 Gy in 3 fractions corresponds to the BED of 43.2 Gy₁₀, which is within the BED range of 37.5-60 Gy₁₀ of the 15-20 Gy single fraction grid regimens. Pollack et al. (2020) reported the use of LRT (12 Gy to 1-3 cylindrical shaped vertices) as upfront boost followed by the conventional

fractionation for favorable to high-risk prostate cancer. The intent of using LRT as a boost for prostate cancer was to improve disease control. The other application of LRT is to induce anti-tumor immunity in combination with immune checkpoint blockade treatment. Jiang et al. (2021) reported a case of complete local tumor response for metastatic non-small cell lung cancer with a single fraction of 20 Gy prescribed to 6 high dose vertices combined with immunotherapy. It is crucial to have valley dose as low as reasonably achievable and minimal valley dose was 2.9 Gy.

For LRT Plans, the maximum doses to the skin for case 2 and case 3 in Table 10 meet the constraint mentioned in AAPM TG-101 but are higher than the other cases because of the superficial extent of the bulky tumor in case 2 and case 3. The bowel dose met the objective but was high because of the bowel inside/abutting the large PTV. The hotspot for all the plans was less than 120% as recommended by Duriseti et al. (2021). The expected mean dose range for PTV_Avoid structure is 19.4 - 23.2 Gy and the mean dose for this structure is within expected range for all test plans. The holes in the dose distribution are visible in the axial plane below 20 Gy in Figure 26 and below 22 Gy for larger targets(>2000 cc) in Figure 28. The expected PVDR which is obtained by dividing the mean dose of PTV_6670 by the mean dose of PTV_Avoid is 3 - 3.7 and the PVDR for all the cases is within expected range and calculated to be slightly smaller for larger targets as the mean dose for PTV_Avoid structure for them is slightly higher. The MU ratio between 2 - 4 is desirable and can be up to 6 for larger targets that are greater than 2000 cc. All the plans met the desired MU ratio criteria.

5) CONCLUSION

The process for commissioning, patient selection, simulation, contouring, and treatment planning of SFRT plans based on previous studies were explored and accurately implemented at ICC. The calculated and measured point doses, and beam profiles at different depths for the physical grid were found to be in clinically acceptable agreements. Grid therapy using physical blocks is a simple planning and delivery technique, which is beneficial to large and advanced tumors and incites rapid tumor response with a large single dose fraction (High PVDR). The limitations associated with this technique include difficulties with dose delivery to deep tissues and poor normal tissue sparing. In contrast, the MLC crossfire technique does not require physical blocks and allows for high target doses to bulky deep-seated lesions while protecting organs at risk. It is a simple and fast forward planning technique, so optimization and patient specific quality assurance are not required. Lastly, the LRT is an inverse planning technique, which is complex but provides flexibility in creating 3D space fractionated dose distributions and provides superior normal tissue sparing compared to grid therapy.

REFERENCES

- 1) Zhang, Hualin et al. "Photon GRID Radiation Therapy: A Physics and Dosimetry White Paper from the Radiosurgery Society (RSS) GRID/LATTICE, Microbeam and FLASH Radiotherapy Working Group." *Radiation research* vol. 194,6 (2020): 665-677. doi:10.1667/RADE-20-00047.1
- 2) Nobah, A et al. "Effective spatially fractionated GRID radiation treatment planning for a passive grid block." *The British journal of radiology* vol. 88,1045 (2015): 20140363. doi:10.1259/bjr.20140363
- 3) Buckey, Courtney et al. "Evaluation of a commercially available block for spatially fractionated radiation therapy." *Journal of applied clinical medical physics* vol. 11,3 3163. 26 Apr. 2010, doi:10.1120/jacmp.v11i3.3163
- 4) Gholami, Somayeh et al. "Is grid therapy useful for all tumors and every grid block design?." *Journal of applied clinical medical physics* vol. 17,2 206-219. 8 Mar. 2016, doi:10.1120/jacmp.v17i2.6015
- 5) Meigooni, Ali S et al. "Dosimetric evaluation of parallel opposed spatially fractionated radiation therapy of deep-seated bulky tumors." *Medical physics* vol. 34,2 (2007): 599-603. doi:10.1118/1.2431423
- 6) Meigooni, Ali S et al. "Dosimetric characteristics of a newly designed grid block for megavoltage photon radiation and its therapeutic advantage using a linear quadratic model." *Medical physics* vol. 33,9 (2006): 3165-73. doi:10.1118/1.2241998
- 7) Kaiser, A et al. "Dramatic response from neoadjuvant, spatially fractionated GRID radiotherapy (SFGRT) for large, high-grade extremity sarcoma." *J Radiat Oncol* 2, 103–106 (2013). doi:10.1007/s13566-012-0064-5
- 8) Laissue, Jean A et al. "Alban Köhler (1874-1947): Erfinder der Gittertherapie" [Alban Köhler (1874-1947): Inventor of grid therapy]. *Zeitschrift für medizinische Physik* vol. 22,2 (2012): 90-9. doi:10.1016/j.zemedi.2011.07.002
- 9) Duriseti, Sai et al. "Spatially fractionated stereotactic body radiation therapy (Lattice) for large tumors." *Advances in radiation oncology* vol. 6,3 100639. 8 Jan. 2021, doi:10.1016/j.adro.2020.100639

- 10) Duriseti, Sai et al. "LITE SABR M1: A phase I trial of Lattice stereotactic body radiotherapy for large tumors." *Radiotherapy and oncology : journal of the European Society for Therapeutic Radiology and Oncology* vol. 167 (2022): 317-322. doi:10.1016/j.radonc.2021.11.023
- 11) Yan, Weisi et al. "Spatially fractionated radiation therapy: History, present and the future." *Clinical and translational radiation oncology* vol. 20 30-38. 22 Oct. 2019, doi:10.1016/j.ctro.2019.10.004
- 12) Wu, Xiaodong et al. "The Technical and Clinical Implementation of LATTICE Radiation Therapy (LRT)." *Radiation research* vol. 194,6 (2020): 737-746. doi:10.1667/RADE-20-00066.1
- 13) Benedict, Stanley H et al. "Stereotactic body radiation therapy: the report of AAPM Task Group 101." *Medical physics* vol. 37,8 (2010): 4078-101. doi:10.1118/1.3438081
- 14) Grams, Michael P et al. "VMAT Grid Therapy: A Widely Applicable Planning Approach." *Practical radiation oncology* vol. 11,3 (2021): e339-e347. doi:10.1016/j.ppro.2020.10.007
- 15) Kavanaugh, James A et al. "LITE SABR M1: Planning design and dosimetric endpoints for a phase I trial of lattice SBRT." *Radiotherapy and oncology : journal of the European Society for Therapeutic Radiology and Oncology* vol. 167 (2022): 172-178. doi:10.1016/j.radonc.2021.12.003
- 16) Pokhrel, Damodar et al. "Conebeam CT-guided 3D MLC-based spatially fractionated radiation therapy for bulky masses." *Journal of applied clinical medical physics* vol. 23,5 (2022): e13608. doi:10.1002/acm2.13608
- 17) Pokhrel, Damodar et al. "A novel, yet simple MLC-based 3D-crossfire technique for spatially fractionated GRID therapy treatment of deep-seated bulky tumors." *Journal of applied clinical medical physics* vol. 21,3 (2020): 68-74. doi:10.1002/acm2.12826
- 18) Mayr, Nina A et al. "An International Consensus on the Design of Prospective Clinical-Translational Trials in Spatially Fractionated Radiation Therapy." *Advances in radiation oncology* vol. 7,2 100866. 11 Dec. 2021, doi:10.1016/j.adro.2021.100866

- 19) Li, Heng et al. "Overview and recommendations for prospective multi-institutional clinical trials of Spatially Fractionated Radiation Therapy (SFRT)." *International journal of radiation oncology, biology, physics*, S0360-3016(23)08246-9. 16 Dec. 2023, doi:10.1016/j.ijrobp.2023.12.013
- 20) Zwicker, Robert D et al. "Therapeutic advantage of grid irradiation for large single fractions." *International journal of radiation oncology, biology, physics* vol. 58,4 (2004): 1309-15. doi:10.1016/j.ijrobp.2003.07.003
- 21) Zhang, Hualin et al. "Fractionated grid therapy in treating cervical cancers: conventional fractionation or hypofractionation?." *International journal of radiation oncology, biology, physics* vol. 70,1 (2008): 280-8. doi:10.1016/j.ijrobp.2007.08.024
- 22) Amendola, Beatriz E et al. "Improved outcome of treating locally advanced lung cancer with the use of Lattice Radiotherapy (LRT): A case report." *Clinical and translational radiation oncology* vol. 9 68-71. 12 Jan. 2018, doi:10.1016/j.ctro.2018.01.003
- 23) Asur, Rajalakshmi et al. "High dose bystander effects in spatially fractionated radiation therapy." *Cancer letters* vol. 356,1 (2015): 52-7. doi:10.1016/j.canlet.2013.10.032
- 24) Amendola, Beatriz E et al. "Spatially Fractionated Radiation Therapy Using Lattice Radiation in Far-advanced Bulky Cervical Cancer: A Clinical and Molecular Imaging and Outcome Study." *Radiation research* vol. 194,6 (2020): 724-736. doi:10.1667/RADE-20-00038.1
- 25) Amendola, Beatriz E et al. "Safety and Efficacy of Lattice Radiotherapy in Voluminous Non-small Cell Lung Cancer." *Cureus* vol. 11,3 e4263. 18 Mar. 2019, doi:10.7759/cureus.4263
- 26) Amendola BE, Perez NC, Wu X, Blanco Suarez JM, Lu JJ, Amendola M. Improved outcome of treating locally advanced lung cancer with the use of Lattice Radiotherapy (LRT): A case report. *Clin Transl Radiat Oncol*. 2018 Jan 12;9:68-71. doi: 10.1016/j.ctro.2018.01.003. PMID: 29594253; PMCID: PMC5862683.
- 27) Grams, Michael P et al. "Clinical aspects of spatially fractionated radiation therapy treatments." *Physica medica : PM : an international journal devoted to the applications of*

physics to medicine and biology : official journal of the Italian Association of Biomedical Physics (AIFB) vol. 111 (2023): 102616. doi:10.1016/j.ejmp.2023.102616

- 28) Price, Alex T et al. "First treatments for Lattice stereotactic body radiation therapy using magnetic resonance image guided radiation therapy." *Clinical and translational radiation oncology* vol. 39 100577. 6 Jan. 2023, doi:10.1016/j.ctro.2023.100577
- 29) Massaccesi, M et al. "Spatially fractionated radiotherapy (SFRT) targeting the hypoxic tumor segment for the intentional induction of non-targeted effects: An in silico study to exploit a new treatment paradigm." *Technical innovations & patient support in radiation oncology* vol. 14 11-14. 2 Mar. 2020, doi:10.1016/j.tipsro.2020.02.003
- 30) Griffin, Robert J et al. "History and current perspectives on the biological effects of high-dose spatial fractionation and high dose-rate approaches: GRID, Microbeam & FLASH radiotherapy." *The British journal of radiology* vol. 93,1113 (2020): 20200217. doi:10.1259/bjr.20200217
- 31) Mohiuddin, M et al. "Palliative treatment of advanced cancer using multiple nonconfluent pencil beam radiation. A pilot study." *Cancer* vol. 66,1 (1990): 114-8. doi:10.1002/1097-0142(19900701)66:1<114:aid-cnrc2820660121>3.0.co;2-1
- 32) Mohiuddin, M et al. "Spatially fractionated (GRID) radiation for palliative treatment of advanced cancer." *Radiation Oncology Investigations* 4 (1996): 41-47.
- 33) Mohiuddin, M et al. "High-dose spatially-fractionated radiation (GRID): a new paradigm in the management of advanced cancers." *International journal of radiation oncology, biology, physics* vol. 45,3 (1999): 721-7. doi:10.1016/s0360-3016(99)00170-4
- 34) Huhn, Jeniffer L et al. "Spatially fractionated GRID radiation treatment of advanced neck disease associated with head and neck cancer." *Technology in cancer research & treatment* vol. 5,6 (2006): 607-12. doi:10.1177/153303460600500608
- 35) Peñagaricano, José A et al. "Evaluation of spatially fractionated radiotherapy (GRID) and definitive chemoradiotherapy with curative intent for locally advanced squamous cell carcinoma of the head and neck: initial response rates and toxicity." *International journal of radiation oncology, biology, physics* vol. 76,5 (2010): 1369-75. doi:10.1016/j.ijrobp.2009.03.030

- 36) Neuner, Geoffrey et al. "High-dose spatially fractionated GRID radiation therapy (SFGRT): a comparison of treatment outcomes with Cerrobend vs. MLC SFGRT." *International journal of radiation oncology, biology, physics* vol. 82,5 (2012): 1642-9. doi:10.1016/j.ijrobp.2011.01.065
- 37) Tubin, Slavisa et al. "Novel stereotactic body radiation therapy (SBRT)-based partial tumor irradiation targeting hypoxic segment of bulky tumors (SBRT-PATHY): improvement of the radiotherapy outcome by exploiting the bystander and abscopal effects." *Radiation oncology (London, England)* vol. 14,1 21. 29 Jan. 2019, doi:10.1186/s13014-019-1227-y
- 38) Kaiser, A et al. "Dramatic response from neoadjuvant, spatially fractionated GRID radiotherapy (SFGRT) for large, high-grade extremity sarcoma." *J Radiat Oncol* 2, 103–106 (2013). doi: 10.1007/s13566-012-0064-5
- 39) Pollack, Alan et al. "Phase I Trial of MRI-Guided Prostate Cancer Lattice Extreme Ablative Dose (LEAD) Boost Radiation Therapy." *International journal of radiation oncology, biology, physics* vol. 107,2 (2020): 305-315. doi:10.1016/j.ijrobp.2020.01.052
- 40) Jiang, Liuqing et al. "Combined High-Dose LATTICE Radiation Therapy and Immune Checkpoint Blockade for Advanced Bulky Tumors: The Concept and a Case Report." *Frontiers in oncology* vol. 10 548132. 12 Feb. 2021, doi:10.3389/fonc.2020.548132

CURRICULUM VITAE

Anupreet Kaur, M.S.
Saraoanu@gmail.com

EDUCATION

Doctor of Medical Physics (DMP)
CAMPEP accredited
University of Nevada, Las Vegas, NV (Aug 2021- May 2024)

Master of Science, Medical Physics (MS)
CAMPEP accredited
San Diego State University, San Diego, CA (Aug 2016- Aug 2018)

Bachelor of Education (B.Ed.)
Punjabi University, Punjab, India (July 2011- May 2012)

Master of Science, Physics (MS)
Panjab University, Chandigarh, India (July 2008 - May 2010)

Bachelor of Science, Physics (BS)
Panjab University, Chandigarh, India (July 2005 - May 2008)

CERTIFICATION

American Board of Radiology PART 1 (August 2018)

NJDEP Qualified Radiological Physicist for Therapeutic Installations (July 2020)

NJDEP Qualified Individual for the Performance of Radiation Safety
Surveys of the Environs for Diagnostic X-Ray Equipment and
Therapy Simulator Systems (July 2020)

CLINICAL EXPERIENCE

THERAPEUTIC MEDICAL PHYSICS

Intermountain Cancer Center, St. George, UT (May 2022 - May 2024)
Radiation Oncology Physics Resident

Medical Physics resident as part of the Doctor of Medical Physics(DMP) program. Responsibilities included Quality assurance of Varian Linear accelerators(Monthly and Annual), GE CT Simulator, and Varian Bravos HDR treatment devices; Assisted in APEX accreditation of site; Patient treatment planning using Eclipse – 3D, IMRT, SRS, SBRT, HDR; weekly chart checks; patient-specific QA; Teaching Radiation therapy students; Implementing spatially fractionated radiation treatment (Lattice and Grid) at the center.

Clinical & Rad Physics, Inc, NJ (June 2018 - Aug 2021)

Providing physics services to Hackensack Meridian Health and New Jersey Urology

Responsibilities included Monthly calibration and QA tests of Varian Linear accelerator; patient-specific QA using SNC Arc check; Review Daily QA test records; initial treatment plan checks with Eclipse; weekly chart checks; Assisted in the Annual calibration of Linac, switch to paperless documentation in Aria, Acceptance tests and Radiation shielding survey on True beam, ACR accreditation of site.

ACADEMIC EXPERIENCE

Teaching Assistant

(Integrated Health Sciences, University of Nevada, Las Vegas, NV) (Aug 2021-May 2022)

Assist with the delivery and evaluation of the course – Introduction to academia and scholarship in health sciences. And help students to get acclimated to the course, and to combat transition challenges.

Teaching Assistant

(Dept of Physics, San Diego State University, San Diego, CA) (Aug 2016-May 2018)

Organized and maintained physics laboratory equipment, demonstrated the operation of equipment to the students, conducted lectures on Electromagnetism by utilizing PowerPoint presentations and white boards to effectively explain the concepts.

PROFESSIONAL ORGANIZATION

AAPM (American Association of Physicists in Medicine)

RSNA (Radiological Society of North America)

ASTRO (American Society for Radiation Oncology)

ABS (American Brachytherapy Society)